Synthesis of Polyaniline HCl Pallets and Films Nanocomposites by Radiation Polymerization

M. A. Ali Omer[1, 2*], E. Saion[2], M. E. M. Gar Elnabi[1] and Kh. Mohd. Dahlan[3]
[1]Sudan University of Science and Technology, College of Medical Radiologic Science,
[2]Department of Physics, Faculty of Science, University Putra Malaysia, Selangor,
[3]Nuclear Agency Malaysia (NAM), Bangi, Selangor,
[1]Sudan
[2,3]Malaysia

1. Introduction

The sources of radiation are so varies, some of them are natural and others are man-made. Also the types of radiation can be categorized according to their wave length or energy or even to the ability of ionizing the media.

Non-ionizing radiation is electromagnetic radiation that does not have sufficient energy to remove the electrons from the outer shell of the atom. Types of non-ionizing radiation are: ultra violet (U/V), Visible light, infrared (IR), microwave (radio and television), and extremely low frequency (ELF, or as they called EMF or ELF-EMF). Non-ionizing radiations produced by a wide variety of sources at homes and in the workplaces, form lasers to power lines, tanning beds to household appliances, cellular phones to home radios (Smith F. A. 2000).

Ionizing Radiation: refer to the types of radiation that has capability to ionize the media directly or indirectly such as X-ray, γ-ray and neutron.

2. Natural sources

The natural sources represented in the following:

i.   Cosmic radiation: represent the radiation comes from outside our solar system as positively charged ions (protons, irons, nuclei, helium…) which are interact with atmospheric layer (air) around the ground to produce secondary radiation as (X-ray, Muons, Protons, Alpha particles, Pions, Electrons and Neutrons).
ii. External terrestrial sources: these represent the radioactive materials, which are found naturally in the earth crust, rocks, water, air and vegetation. The major radio-nuclides found in the earth crust are (Potassium-40, Uranium-235, and Thorium-210).

3. Artificial sources

The main sources of manmade radiation that expose the public are from (Medical Procedures, as in diagnostic X-ray, radiation therapy, nuclear medicine and sterilization).

The common radioactive elements are I-131, Tc-99m, Co-60, Ir-192, St-90 and Cs-137). Other sources exemplar in occupational and consumption products, these implies the radiation in mines, combustible fuel (gas, coal), ophthalmic glasses, televisions, luminous, watch's dial (tritium), X-ray at air-port (detectors), smoke detectors (americium-241), road construction materials, electrons tubes, and fluorescent lamp starters, nuclear fuel cell, nuclear accidents and nuclear weapons in marshal island and war. The yield of artificial sources either as quantum represented in X-ray and gamma radiation (γ) or as particles with high energy as beta particles (β), alpha particles (α), neutrons and electrons. The common artificial sources are accelerators and nuclear reactors (Smith F. A. 2000).

All of the above radiation types were used in researches; today the most common radiation sources applied in researches and in man serves are:

i.   Co-60, as artificial source for gamma (γ) radiation.
ii. Linear accelerators for photon and electron beams, with energy range of (0.3-10 MeV and up to 20 MeV).

These energies are insufficient to initiate nuclear reaction; hence the irradiated element does not exhibit any radioactivity, see the table of radiation sources (1).

Table (1) shows the sources of radiation (Smith, 2000)

Category	Source
Nuclear power	^{235}U fission products, ^{90}Sr, ^{137}Cs
Occupational exposure	X-ray, Isotopes for (γ) ray
Weapons tests	^{235}U, ^{239}Pu, fission products
Every day sources	Coal, Tobacco and Air-travel
Medical tests & treatment	X-ray, (γ)radiation & electrons
Cosmic rays	Protons, electrons, neutrons
Food	40K, 137Cs, 14C and 131I
Rocks & building	235U, 238U, and 232Th
Atmosphere	222Rn and 137Cs

Table 1.

Ionizing radiation is a broad energetic spectrum of electromagnetic waves or high velocity atomic or subatomic particles. The radiation can be categorized according to their ability to ionize the media. Non-ionizing radiation is electromagnetic radiation that does not have sufficient energy to remove an electron of the atom. The various types of non-ionizing radiation are ultra violet (UV), visible light, infrared (IR), microwaves (radio and television), and extremely low frequency (ELF, or as they called EMF or ELF-EMF). Ionizing radiation is electromagnetic radiations, such as X-rays, γ-rays and charged particles (electrons, β-particles and α-particles) which possess sufficient energy to ionize an atom by removing at least an orbital electron. According to the 1996 European Guideline of the European Atomic Energy Community (EURATOM), electromagnetic radiation with a wavelength of 100 nm or less is considered as ionizing radiation which is corresponds to ionizing potential of 12.4 eV or more (Smith, 2000). The ionization potential is dependent on the electronic structure of the target materials and generally in the order of 4 – 25 eV.

The International Commission of Radiation Units (ICRU) has subdivided the ionizing radiation into direct and indirect ionizing radiation, based on the mechanisms by which they ionize the atom. *Direct ionizing radiations* are fast charged particles, such as alpha particles, electrons, beta particles, protons, heavy ions, and charged mesons, which transfer their energy to the orbital electron directly and ionize the atom by means of Columbic force interactions along their track. *Indirect ionizing radiations* are uncharged quantum, such as electromagnetic radiations (X-rays and γ-rays), neutrons, and uncharged mesons, which undergo interactions with matter by indirectly releasing the secondary charged particles which then take turn to transfer energy directly to orbital electrons and ionize the atom. Some properties of ionizing radiation are shown in Table 2. Table (2) shows the properties of different ionizing radiation.

Characteristics	Alpha	Proton	Beta or electron	Photon	Neutron
Symbol	$^4_2\alpha$ or He^{+2}	^1_1p or H$^+$	$_{-1}e$ or β	γ- or X-rays	^1_0n
Charge	+2	+1	-1	Neutral	Neutral
Ionization	Direct	Direct	Direct	Indirect	Indirect
Mass (amu)	4.00277	1.007276	0.000548	-	1.008665
Velocity (m/s)	6.944×10^6	1.38×10^7	2.82×10^8	2.998×10^8	1.38×10^7
Speed of light	2.3%	4.6%	94%	100%	4.6%
Range in air	0.56 cm	1.81 cm	319 cm	820 m	39.25 cm

1 atomic mass unit (amu) = 1.6×10^{-27} kg.
Speed of light c = 3.0×10^8 m/sec.

Table 2. The properties of different ionizing radiation

4. Gamma ray (γ-ray) interaction and attenuation coefficients

In general the characteristic of radiation interaction with matter represented in photoelectric (*Predominates for photons in the low energy range between 10 keV and 200 keV*), Compton (*Predominated at energies of 100 keV - 10 MeV.* (McGervey, 1983)), Pair production (*Predominated at energies greater than twice the rest mass of an electron,* i.e. $2m_0c^2$ = 1.022 MeV, *where m refers to mass of electron and c refers to speed of light* (Johns and Cunningham 1983)), Triplet production process (*occurs when the incident photon have an energy of* $4m_0c^2$, *i.e. it implies both the pair production at the nucleus level plus triplet production*) and Raleigh scattering (*predominant for photons at low energy range from 1 keV to 100 keV*) table (3), is that each individual photon is absorbed or scattered from the incident beam in a single event. The photon number removed ΔI is proportional to the thickness traveled through Δx and the initial photon number I_0, i.e. $\Delta I = -\mu I_0 \Delta x$, where, μ, is a constant proportionality called the attenuation coefficient. In this case, upon integrating, we have the following equation (1)

$$I = I_o e^{-\mu x} \tag{1}$$

The attenuation coefficient is related to the probability of interaction per atom, i.e. the atomic cross section σ_a is given by equation (2)

$$\mu = \frac{\sigma_a N_A \rho}{A} \tag{2}$$

where A is the mass number and N_A the Avogadro's number (6.022×10^{23} mol/1).

Table 3 briefly summarized the entire γ-radiation photon interactions with their possible energies required to initiate the reactions (Smith, 2000; Siegbahn, 1965).

Process	Type of interaction	Other names	Approximate E of Maximum importance.	Z dependence
Photoelectric	With bonded electrons, all E given to electron		Dominant at low E (1-500) KeV, cross section decrease as E increase	Z^3
Scattering from electrons coherent	With bond atomic electron, with free electrons	Rayleigh electron, resonance scattering, Thomson scattering	<1MeV and greatest at small angles. Independent of energy	Z^2, Z^3 Z Z
Incoherent	With bond atomic electron, with free electrons	Compton scattering	<1MeV least at small angle. Dominate in region of 1 MeV, decreases as E increase	Z Z^2
Pair Production	In Coulomb field of Nucleus	Elastic Pair production	Threshold ~1MeV, E > 5MeV. Increase as E increase.	Z
Pair production Delbruk scattering	In coulomb field of electron & nucleus	Triplet production inelastic pair production. Nuclear potential scattering	Threshold at 2 MeV increases as E increases. Real Max > imaginary, below 3 MeV(both increase as E increases)	Z^4

Table 3.

The essence of γ-radiation interaction with molecules and the induction of physical and chemical characteristics that leading to form new compound is ascribed to the amount of energy being transferred, which will create ion, free radicals and excited molecule. Such interaction process is termed ionization and excitation of the molecules, which can cause chemical changes to the irradiated molecule. This is due to the fact that all binding energy for organic compound in the range of 10 – 15 eV. In case of low transferred energy by photon, the molecule undergoes excitation state before returning to the rest state by emitting X-ray photons or break down to release free radicals which in turn undergoes polymerization.

The ejected electron from the irradiated molecule (A^+) is subjected to the strong electric field of the formed positive charge. Therefore the recombination is a frequently occur, either during irradiation or after the end of irradiation to create energetic molecule (A^{**}). Such highly energetic excited molecule will break down into free radicals and new molecule (Denaro, 1972). The fundamental of this reaction can be shown in the following scheme Figure (1).
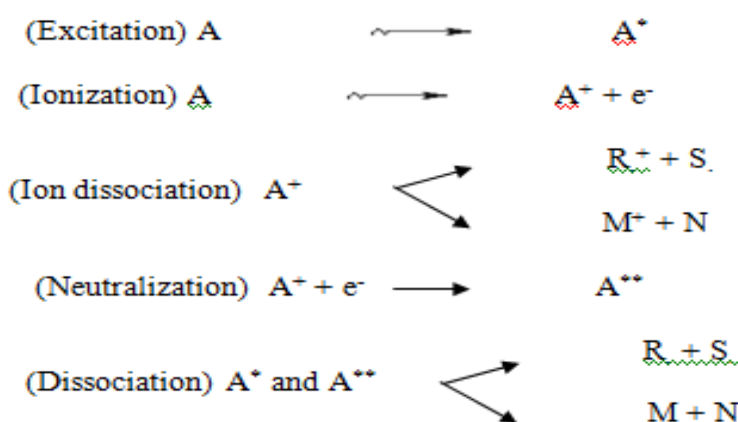

Fig. 1. The expected irradiation results of the organic molecules, where R and S are free radicals and M and N are molecular products.

5. Radiation polymerization

Radiation polymerization is a process in which the free radicals interact with the unsaturated molecules of a low molecular unit known as monomer to form high molecular mass polymer or even with different monomers to produce crosslink polymer. The formed polymer can be in different forms called homopolymer and copolymer depending on the monomer compositions link together. Radiation-induced polymerization process can be achieved in different media whether it is liquid or solid unlike the chemical polymerization which can only accomplished in aqueous media. It is also temperature independent. Radiation polymerization often continues even after removing away from the radiation source. Such condition is known as post-polymerization (Lokhovitsky and Polikarpov, 1980). Since radiation initiation is temperature independent, polymer can be polymerized in the frozen state around aqueous crystals. The mechanism of the radiation induced polymerization is concerning the kinetics of diffusion-controlled reactions and consists of several stages: addition of hydroxyl radicals and hydrogen atoms to carbon-carbon double bond of monomer with subsequent formation of monomer radicals; addition of hydrated

electrons to carbonyl groups and formation of radical anion of a very high rate constant and the decay of radicals with parallel addition of monomer to the growing chain.

6. Cross linking

The process of crosslink occurs due to interaction between two free radical monomers which combine to form intermolecular bond leading to three dimensional net of crosslinked highly molecular polymer, more likely dominate in unsaturated compound or monomer. The crosslinked polymer show strong mechanical strength and high thermal resistance.

7. Radiation grafting

Radiation grafting is a process in which active radical sites are formed on or near the surface of an exciting polymer, followed by polymerization of monomer on these sites. Grafting is accompanied by homopolymerization of the monomer; the material to which the monomer is grafted is described as the backbone, trunk or support. Radiation grafting is used to modify the polymers texture such as film, fibers, fabrics and molding powders. The process of grafting can be expressed as follow; suppose the polymer A is exposed to γ-rays, thus the active free radical sites A* created randomly along the polymer backbone chain, this free radical initiate a free radical on the monomer B then undergoes grafting polymerization at that active sites. The extension of the attached monomer B upon the base polymer A is termed as the degree of grafting DOG which refers to the mass of the grafted polymer as a percentage of the mass of the original base polymer. Such process can be expressed in schematic Figure (2).
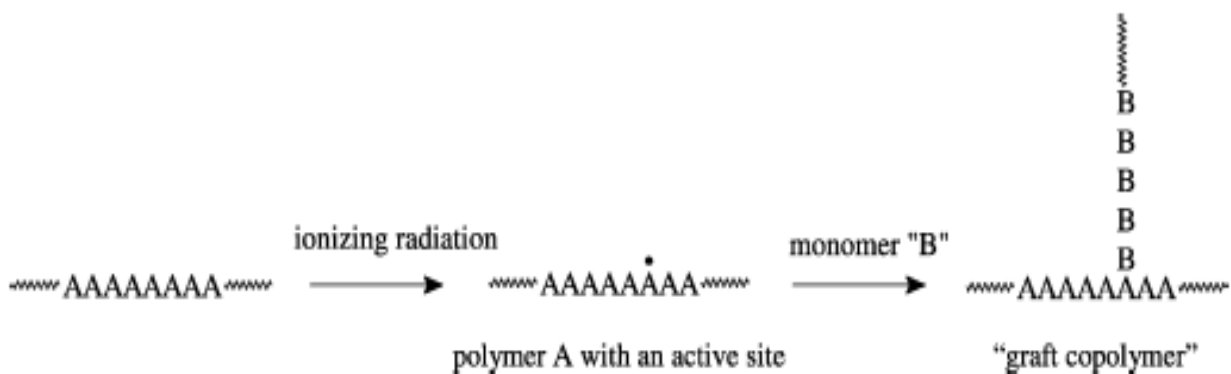

Fig. 2. Schemes for grafting process for polymer A with monomer B using gamma radiation.

Conducting polymers and their composites exhibit excellent optical, electrical, and electrochemical properties and therefore they have potential applications in enhancement the electrode performance of rechargeable batteries and fuel cells, electric energy storage systems in supercapacitors, solar energy conversion, photoelectrochromics, corrosion protection, electromagnetic interference shielding and biosensors (Malinauskas *et al.*, 2005).

In this work attempts are made to produce conducting polyaniline (PANI) formed in pallets and dispersed in PVA matrix (films) then their structure, optical properties and electrical conductivity are investigated. However, for the first time the polymerization of pure PANI

is fully achieved by ionizing radiation (Mohammed, 2007). The prime advantage of radiation processing in this work is that no oxidizing agent is used to polymerize the conducting PANI i.e. giving pure product.

8. Conducting polyaniline nanoparticles

PANI has high electrical conductivity that can be controlled by oxidation or protonic doping mechanism during synthesis. PANI is known for its excellent thermal and environmental stability but poor processibility due to insolubility in most common solvents and brittleness that limits its commercial applications. In the composites form with another water soluble polymers such as PVA, poly(vinyl pyrrolidone), poly(acrylic acid) and poly(styrene sulfonic acid) (PSSA) which used as stabilizers, the processibility of PANI could be improve and a functionalized protonic acid can be added into the composites to chemically polymerize PANI. The PANI dispersion can then be cast to form composite film containing PANI nanoparticles. To improve the conductivity further, chemically and electrochemically PANI/ polymer composites have been irradiated with x-rays, gamma radiation, and electron beams (Bodugoz *et al.*, 1998; Sevil *et al.*, 2003; Wolszczak *et al.*, 1996 a and b; Angelopous *et al.* 1990). When ionizing radiation interacts with polymer materials active species such as ions and free radicals are produced and thus, improved the PANI conductivity.

Conducting PANI has been synthesized by chemical and electrochemical methods, which the later is considered the common one because of better purity. Chemically and electrochemically synthesized polyaniline are subjected to many shortcomings such as impurities, solvent toxicity, long tedious process, poor compatibility, insoluble, expensive, low production and difficult in their preparation, etc. However, report on synthesis of PANI nanoparticles using only γ-irradiation has not been reported until the date of 2007. The advantages of radiation processing is that no metallic catalyst, no oxidizing or reducing agent is needed, synthesis in a solid-state condition, fast and inexpensive, and controllable acquisitions. The synthesis of PVA/PANI nanoparticles by γ-irradiation doping is proposed in this work.

9. Methodology

9.1 Materials and equipments

The materials used for preparing the samples in this study, namely as polyvinyl alcohol PVA, aniline hydrochloride AniHCl, γ-radiation as an effective tool for polymerization process and reducing agent, Petri-dishes, micrometer, UV-spectroscopy, Raman spectroscopy and LCR-meter.

9.2 Method

The Aniline hydrochloride AniHCl monomer as 2.5, g (28.6 W/V) has been dissolved in distill deionized water of 100 ml under nitrogen atmosphere and bubbling in the solution with continuous stirring using magnetic stirrer for 3 hour. Then the solution has been irradiated with γ-radiation receiving 10, 20, 30, 40 and 50 kGy. The polymerized AniHCl i.e. polyaniline PANI-HCl has been precipitated filtered and collected in a form of powder. The powder (2.5g) pressed by 10 tons to form pallets.

On the other hand a polyvinyl alcohol (PVA) was supplied by SIGMA (Mw = 72,000 g/mol, 99 – 100% hydrolyzed) has been prepared by dissolving 30.00 g PVA powder in 600 ml distilled deionized water at controlled temperature of 80 °C in the water-bath. The solution was magnetically stirred throughout at that temperature for 3 hours and then left to cool at room temperature. After cooling to room temperature, a weight of AniHCl, 2.5, g was added into 100 ml PVA solution, which gives the AniHCl concentrations as 28.6, wt%, by weight in comparison to the PVA. The mixtures were stirred continuously for 10 hours using a magnetic stirrer in nitrogen atmosphere. Then the PVA/AniHCl blend solution has been irradiated by γ-radiation receiving 10, 20, 30, 40 and 50 kGys and after irradiation the solution has been divided into Petri-dishes, each contains 20 ml and left to dry at ambient temperature and dark room for 3 days to evaporate the water. The casting film was pealed off and cut into several pieces which were eventually packed in a sealed black plastic bag.

Fig. 3. The UV-visible spectrophotometer model Camspec M530.
Faculty of Science, Department of Physics-UPM

Fig. 4. Raman system and its accessories for sample set up and characterization,
Faculty of Science, department of Physics - UPM

The thickness of the films was determined by a digital micrometer model Mitutoyo no: 293-521-30-Japan, The average thickness of the films was 2 mm, and then the products (Films of PANI-HCl and pallets) have been characterized using the following instrument:

Fig. 5. The LCR-meter model HP 4284A with the sample set up for conductivity measurement. Faculty of Science, department of Physics - UPM

Fig. 6. γ-irradiation system model (J. L. Sherperd) at the Malaysian Nuclear Agency, Bangi - Malaysia UPM

10. Results and discussion

Figure 7 shows the prepared PVA solution (a), AniHCl\PVA solution (b). And AniHCl\PVA solution irradiated with 50 kGy γ-radiation doses (c). It shows that the PVA is a soluble in water appears as clear glycerin like material and after the dissolving of AniHCl

it shows the oily color and after an irradiation with 50 kGy the color turned to dark green solution, which is the color of polyaniline PANI. While Fig. 7-d shows the pur pallets of PANI-HCl and the formed films of PVA\ PANI-HCl (e). These obtained materials have been subjected for further characterization.

Upon irradiation, the PVA/AniHCl blend films with doses up to 50 kGy, γ-rays interacts with the PVA binder liberating electrons by photoelectric effect and Compton scattering and followed by ions of H^+ and OH^- from the bond scission. However, the contribution of these ions to the final product is not very significant. On the other hand, the interaction of γ-rays with the AniHCl is dominant due to the fact that HCl is easily dissociated to H^+ and Cl^- ions by radiation. The protonation of aniline monomer by Cl^- produced conducting PANI nanoparticles which can be visualized by the change of color of the un-irradiated PVA/AniHCl blend film from colorless to dark green at 50 kGy, as illustrated by the photograph pictures in Figure 5.14. As mention earlier, the formation of C=N double bonds of imines group produced green colour of PANI and the intensity increases with increasing of dose (*see Raman spectrum*). Before irradiation, all PVA/AniHCl blend films were colourless even exposed in air, suggesting the UV-visible radiation has no influence in the formation of conducting PANI. Only after irradiation with the dose between 20 kGy and 50 kGy, the green colour became intense.

50.0 kGy   40.0 kGy   30.0 kGy   20.0 kGy   10.0 kGy   00.0 kGy
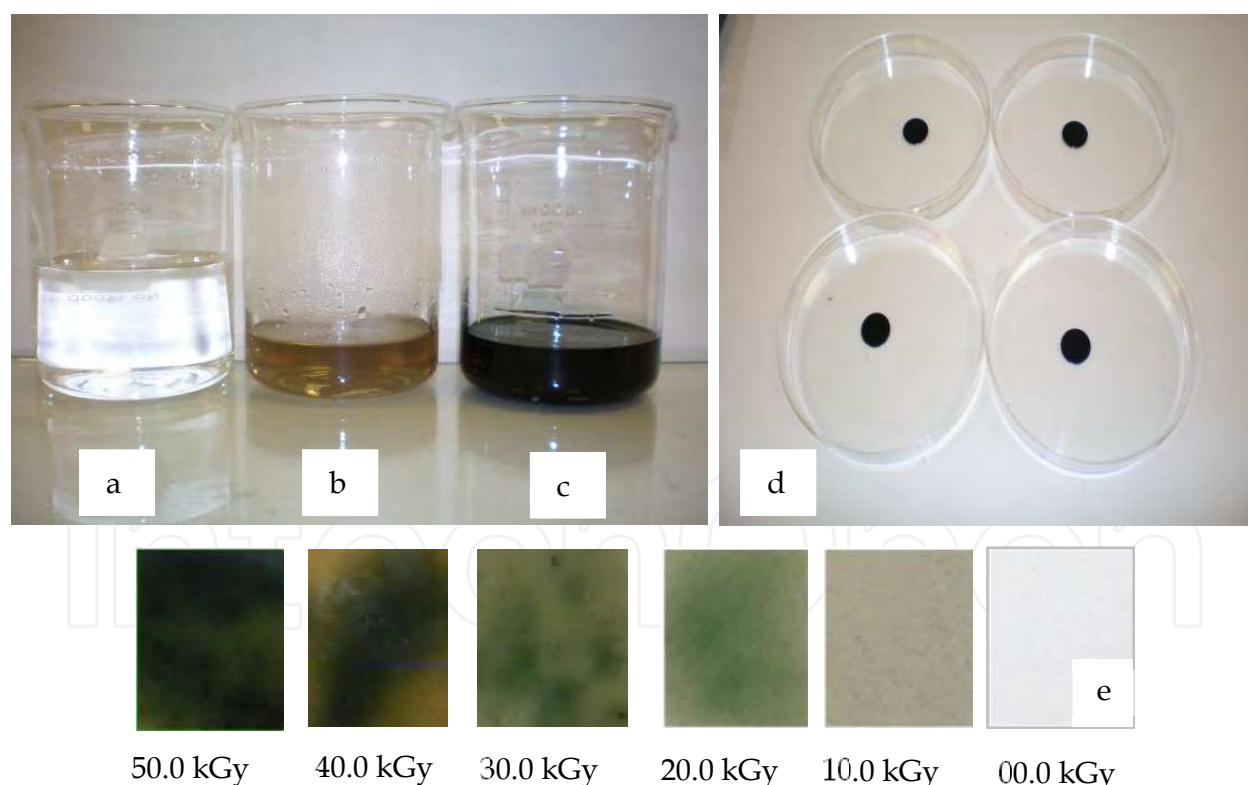
Fig. 7. Shows the prepared PVA solution (a), AniHCl\PVA solution (b), AniHCl\PVA solution irradiated with 50 kGy γ-radiation dose (c), the PANI-HCl pallets (d) and the formed films of PANI-HCl at different radiation doses.

Figure 8 shows the UV-visible absorption spectra of an irradiated AniHCl\PVA composite at different radiation doses at 0, 10, 20, 30, 40, and 50 kGy and for a concentration of 28.6

wt% AniHCl formed as films. The optical absorption spectra of the irradiated films were measured by using UV–Visible double beam spectrophotometer with air as a reference. The optical absorption is a useful tool to study electronic transitions in molecules, which can provide information on band structure and band gap energy. The basic principle is that photons from UV-visible light source with energies greater than the band gap energy will be absorbed by the materials under study. The absorption is associated with the electronic transitions from highly occupied molecular orbital (HOMO) π-band to lowly unoccupied molecular orbital (LUMO) π*-band of electronic states (Arshak and Korostynska, 2002). The electronic transitions between the valence band (VB) and the conduction band (CV) start at the absorption edge, which corresponds to the minimum energy of band gap E_g between the lowest minimum of the CB and the highest maximum of the VB.
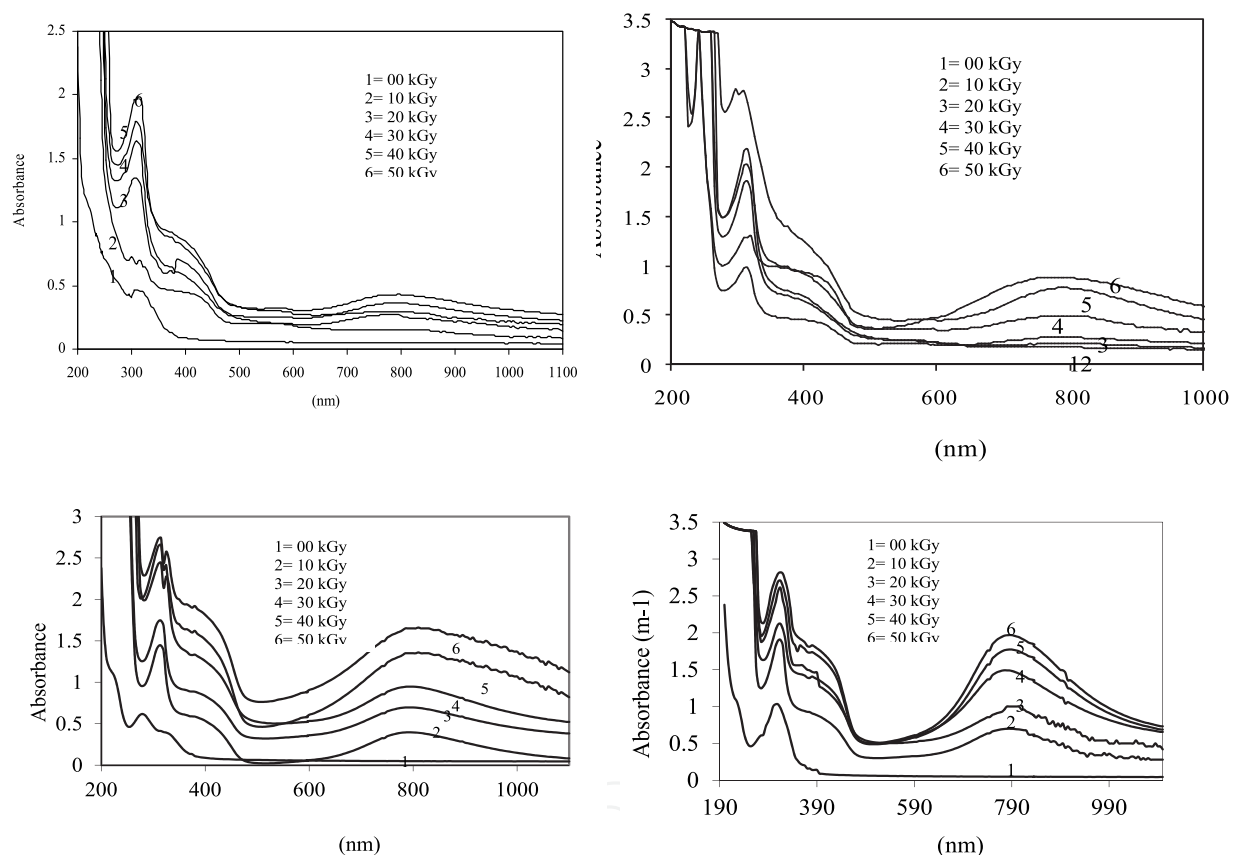
Fig. 8. Shows the UV-visible absorption spectra of PANI nanoparticles dispersed in PVA matrix for AniHCl monomer concentrations of (a) 9, (b) 16.7, (c) 23, and (d) 28.6 wt%.

The spectra of irradiated films reveal two prominent absorption peaks at 315 and 790 nm assigned to the electronic transitions of chlorine Cl- and C=N bond respectively. The absorbance corresponds to the excitation of outer electrons through π-π* electronic transitions at the bands of 315 nm (3.95 eV) and 790 nm (1.57 eV). The absorbance increases with the increase of dose and AniHCl concentration and both peaks become sharper with dose increase, indicating the amount of Cl- and polarons formed (represented by C=N) have increased with dose increase. Both peaks shifted slightly to higher wavelengths with the increase of dose but were not very significant.

The absorbance at 790 nm is due to the creation of C=N double bond of imines group representing the polarons in conducting PANI that gives the green colour. This result is in agreement with previous study carried out by Rao, *et al*. (2000), in which the absorption band for the chemically prepared conducting PANI salt peaking in the range of 420 – 830 nm depending on the degree of oxidation. Earlier Malmonge and Mattoso (1997) found that the absorption band of chemically synthesized PANI was 630 nm and when exposed to X-rays, the peak became sharper and shifted to 850 nm leading to an increase of the conductivity. Recent study by Cho *et al*. (2004) showed that the absorption bands were peaking at 740 – 800 nm for PANI chemically prepared by hydrochloric acid doping and dispersed in PVA matrix.

The unirradiated PVA/AniHCl film showed a broad peak at 315 nm because of the presence of Cl- in AniHCl monomer and no other peak is visible in UV region. The peak increases in intensity at higher concentration of AniHCl monomer. As the dose increases the absorbance at 315 nm increases due to increased formation of chlorine Cl- ions from the dissociation of HCl. Solid phase of HCl was present as the residual of radiation doping of imines group which can be seen from SEM micrographs in Figure 5.4. De Albuqerque, *et al*. (2004) measured UV-Visible spectra of emeraldine salt solution and found two absorption peaks at 320 nm and 634 nm. The presence of the absorption peak at 315 nm has been reported by Azian (2006) for irradiated PVA/AniHCl composites below 20 kGy and was confirmed by the UV-Visible spectroscopy measurements on HCl solution.

11. Quantitative analysis formation of PANI composites

Figure 9 shows the absorbance at 790 nm band for conducting PANI composites that increases exponentially with dose and can be fitted to the theoretical relationship of the form:

$$y = y_0 \exp(D / D_0) \tag{3}$$

where y is the absorbance at dose D, y_0 is the absorbance at zero doses and D_0 is the dose sensitivity parameter.

The exponential increase of absorbance of PANI nanoparticles turns out to be of similar trend with the exponential increase of C=N formation determined from the Raman scattering measurement. This indicates the same phenomenon measured by two different methods produces almost similar result. Thus, the quantitative analysis of polarons could be extracted by either the Raman scattering or the optical absorbance method. The values of D_0 from the absorbance of PANI composites at different AniHCl concentrations were determined from the inverse of the gradient ln y vs. dose, as shown in Figure 9 and plotted for different AniHCl concentrations. The result shows a decrease in the D_0 value with the increase of AniHCl concentration. Thus, the PVA/PANI composites became more radiosensitive at higher AniHCl concentration as shown in Figure 10. The linear relationship between D_0 and AniHCl concentration C is $D_0 = -0.29C + 23.7$.
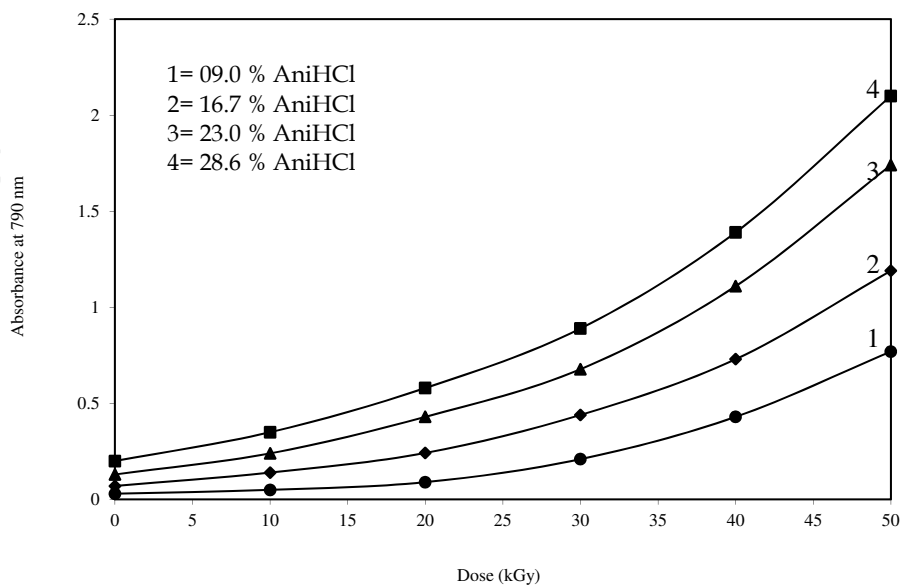
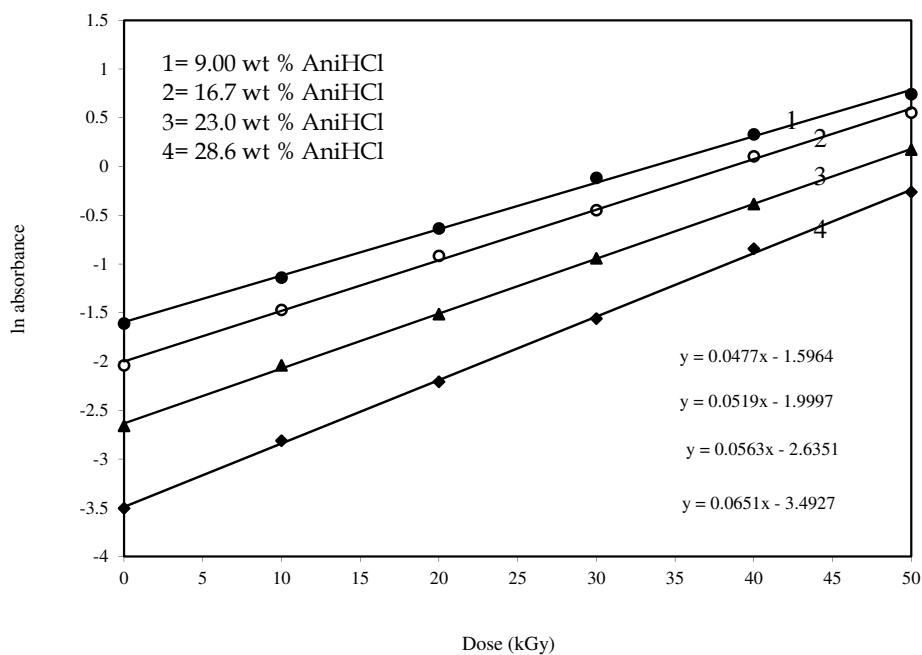Fig. 9. Shows the exponentially increment of absorbance at 790 nm due to the formation of PANI

Fig. 10. Shows the ln (log$_e$) absorbance (ln y) vs. dose at different AniHCl concentrations and the gradient is used to determine the dose sensitivity D_0.
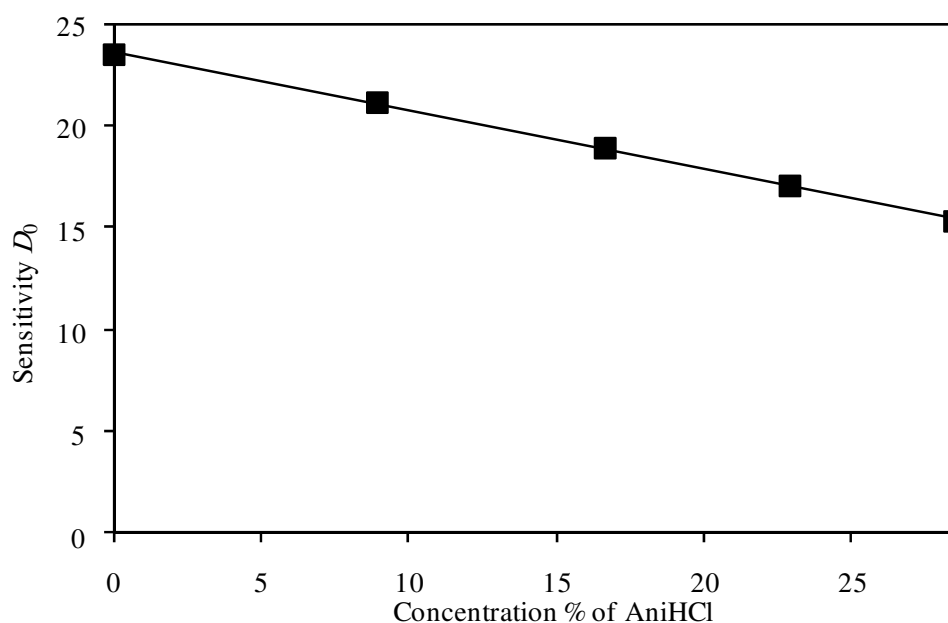
Fig. 11. Shows the deduction of Dose sensitivity D_0 of PANI nanoparticles versus AniHC concentration

12. Quantitative analysis of HCl formation

Figure 12 shows the absorbance at 315 nm band due to the formation of HCl versus radiation dose. The absorbance increases exponentially following the radiation dose increment and leading to saturation at doses higher than 50 kGy, indicating chlorine ions Cl⁻ were being consumed for the formation of conducting PANI composites. The relation between the absorbance of Cl⁻ and dose could be fitted to the relation of the form:

$$y = A_0(1 - \exp(-D/D_0))$$ (4)

where y is the absorbance at the applied dose D for each concentration, A_0 is the difference between the absorbance at 50 kGy and 0 Gy for each concentration. The values of D_0 for the formation of crystalline HCl at different AniHCl concentrations can be determined from the inverse of the gradient $\ln\left(1 - \dfrac{y}{A_0}\right)$ versus dose, as shown in Figure 13. The values of D_0 at different AniHCl concentrations are shown in Figure 14 which can be written in the form $D_0 = 15.75\ C + 14.456$.
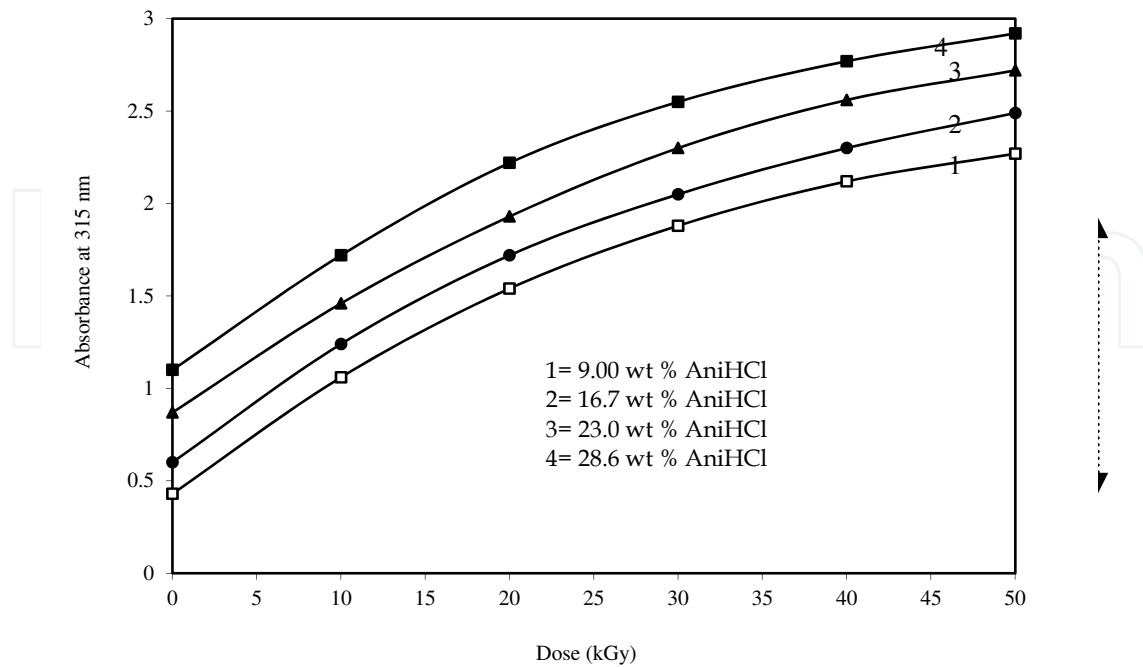
Fig. 12. Shows the absorbance at 315 nm for the consumption of Cl⁻ in composite PVA/PANI nanoparticles vs. radiation dose.
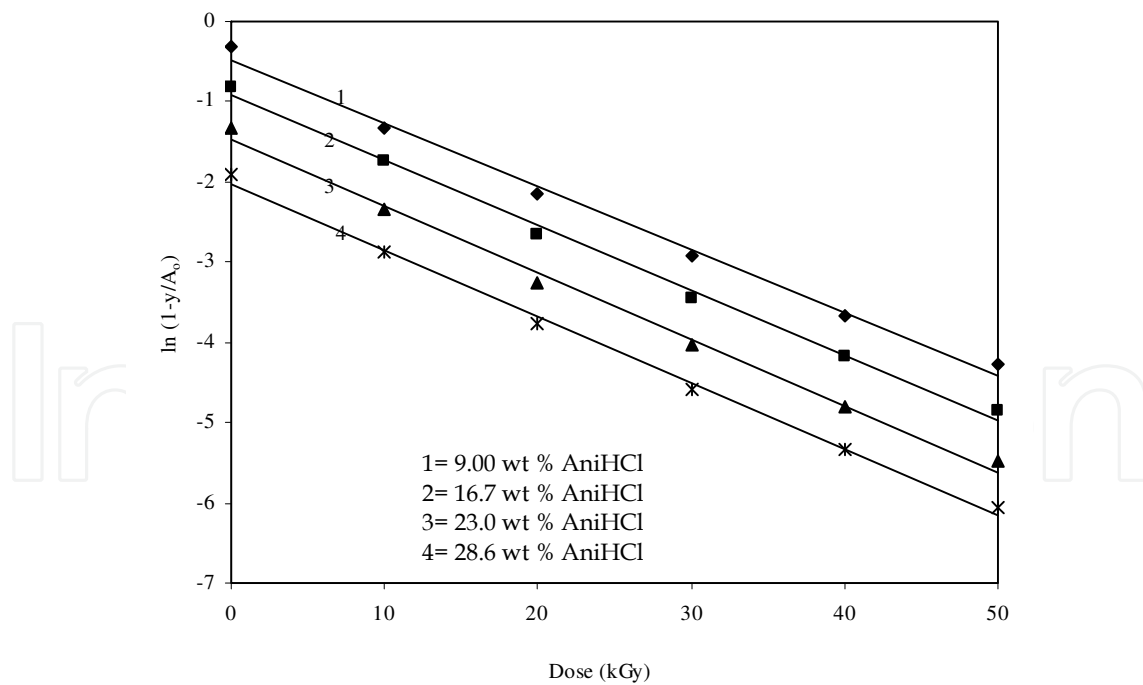
Fig. 13. Shows the $\ln\left(1 - \dfrac{y}{A_0}\right)$ versus dose for consumption of Cl⁻ at different AniHCl concentrations to deduce the dose sensitivity D_0.
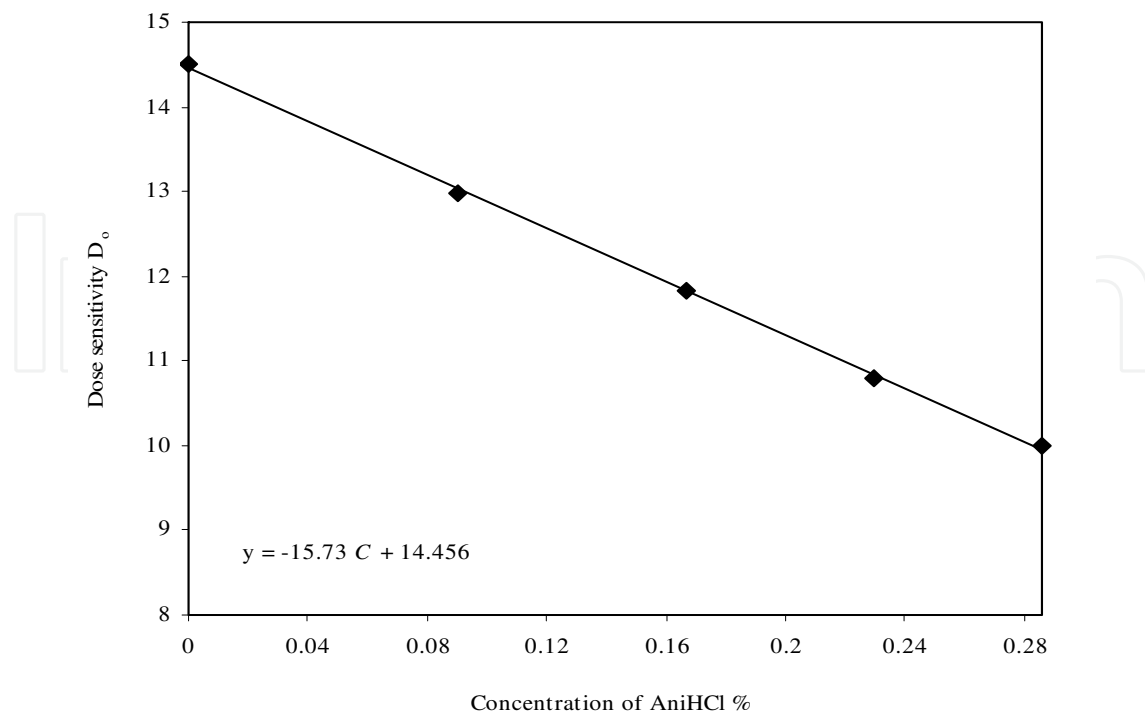
Fig. 14. Shows the dose sensitivity D_0 of composite of PVA/PANI nanoparticles versus monomer concentration for consumption of Cl⁻

13. Band gap of PANI nanoparticles

At high absorption level, $\alpha > 10^4$ cm⁻¹, the absorption coefficient $\alpha(v)hv$ is related to the band gap E_g according to the Mott and Davis (1979) using the following relation:

$$\alpha(v)hv = B(hv - E_g)^m \tag{5}$$

where, hv is the energy of the incidence photon, h is the Planck constant, E_g is the optical band gap energy, B is a constant known as the disorder parameter which is dependent on composition and independent to photon energy. Parameter m is the power coefficient with the value that is determined by the type of possible electronic transitions, i.e.1/2, 3/2, 2 or 1/3 for direct allowed, direct forbidden, indirect allowed and indirect forbidden respectively. The band gap denotes the energy between the valence bands (VB) and the conduction band (CB). The direct allowed band gap at different doses were evaluated from the plot of $(a(v)hv)^2$ vs. hv. By extrapolation a straight line of $a(v)hv)^2$ versus hv curves for $(a(v)hv)^2 = 0$, the band gap can be determined as shown in Figure 15. The results showed that band gap E_g value decreases with the increase of the radiation dose shown in Figure 16. The decrease in the band gap energy with increasing dose is attributed to more conducting PANI nanoparticles formed and as more polarons in the irradiated composite reduce the band gap between VB and CB for the $\pi - \pi^*$ electronic transition. We found that when the doses were increased from 10 to 50 kGy the band gap decreases from 1.36 to 1.18 eV for 9 wt %, from 1.28 to 1.09 eV for 16.7 wt %, from 1.21 to 1.04 eV for 23 wt % and from 1.12 to 1.00 eV for 28.6 wt %.
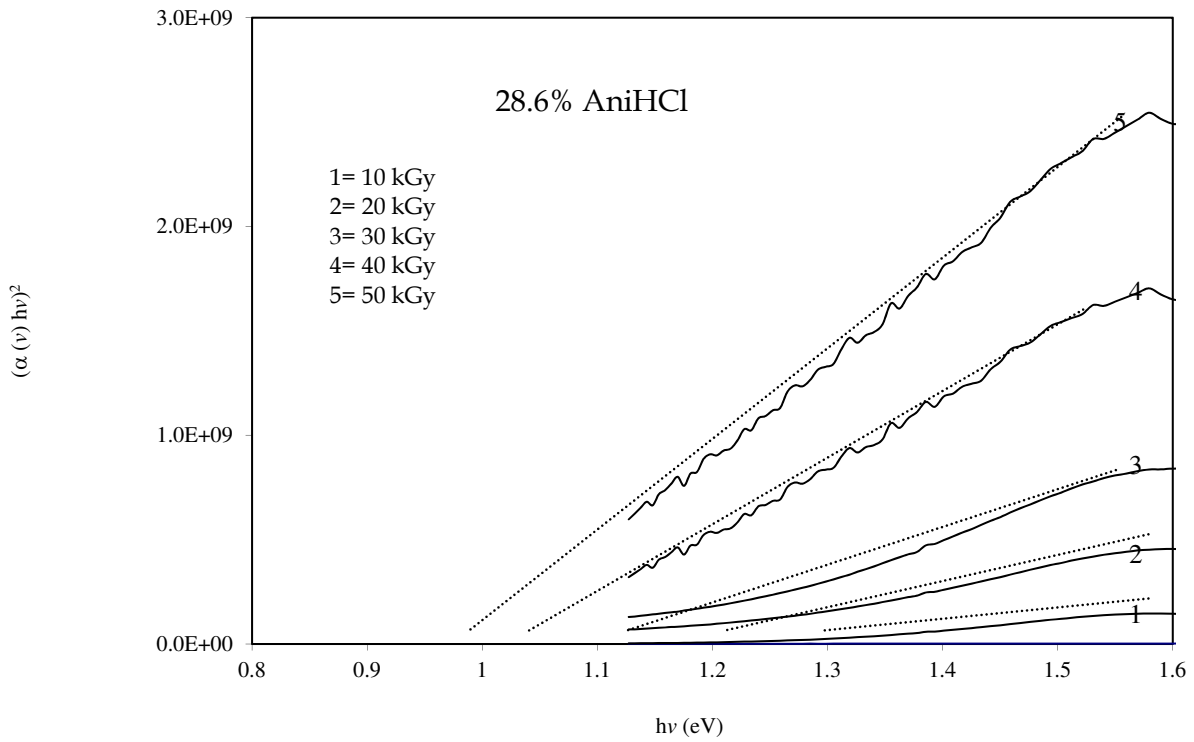
Fig. 15. Shows Variation of direct allowed energy gap for AniHCl monomer concentrations of 28.6 wt% at different doses (example for plot of $(a(v)hv)^2$ vs. hv. By extrapolation a straight line of $a(v)hv)^2$ versus hv curves for $(a(v)hv)^2 = 0$)
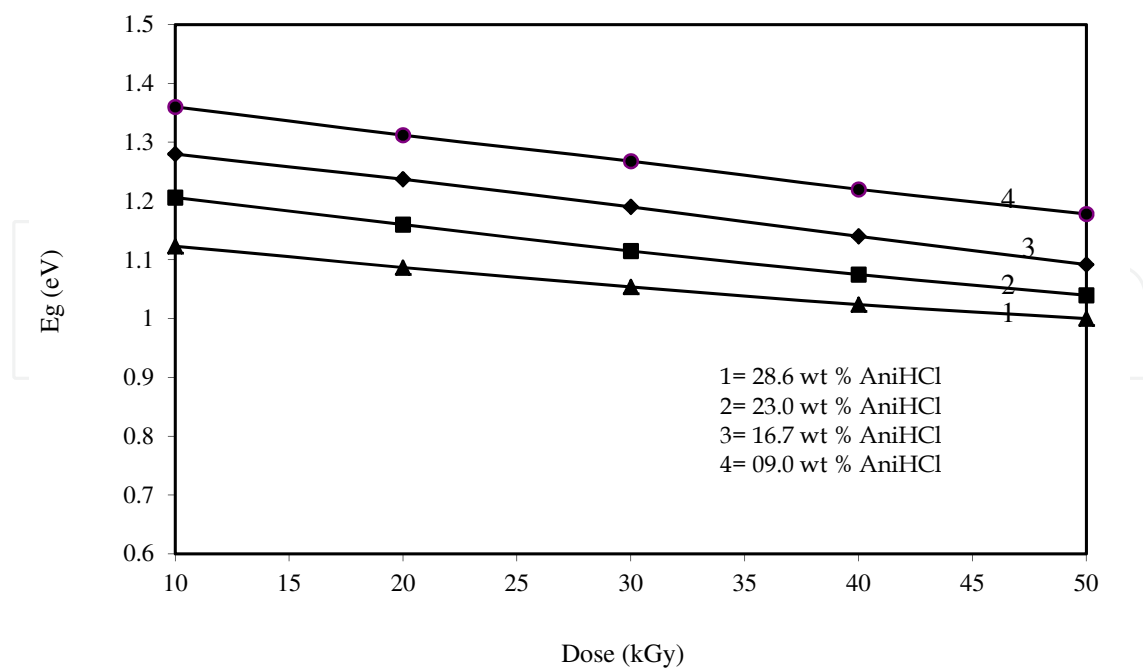

Fig. 16. Shows the band gap energy E_g vsersus dose for PANI composites at different monomer concentrations

14. Electrical conductivity of composite of PVA/PANI nanoparticles

Polymers are commonly insulators as they have no significant mobile charges to serve the electrical conductivity. One of the requirements for polymers to exhibit good conductivity is the existence of π-electrons, which overlaps along the conjugated chain to form π-conjugated band. The conductivity of conjugated polymers or pure polymers can be increased after suitable oxidization or reduction process (Kanazawa *et al.*, 1979; Blythe, 1979) by doping or blending with charge donors of several organic groups (El-Sayed *et al.*, 2003) like hydroxyl, amine, carboxylate, sulfonate, and quaternary ammonium (Blanco *et al.*, 2001) or by radiation induced doping (Park *et al.*, 2002). In this work, the PVA was first blended with the organic monomer, AniHCl and then followed by γ irradiation to oxidize the monomer into the conducting PANI.

The conductivity of polymer composites, generally consist of free or weakly bound electronic and ionic charges and trapped ionic charges in the polymer matrix. The free charges are free to move in electrical field, independent of frequency and contribute to the direct current (dc) conductivity. While charge carriers that are trapped in the polymer matrix require alternating electric field at certain frequency to liberate the ions from one site to another site in succession by hopping mechanism and contribute to the alternating current (ac) conductivity. Realizing this, the electrical conductivity of un-irradiated and irradiated PVA will be measured and discussed first. This allows us to determine the conductivity values and identify the type of charge carriers in the un-irradiated and irradiated PVA before blending the PVA with AniHCl monomer at various concentrations and undergo γirradiation.

15. Conductivity of PVA/AniHCl composite at various concentrations

Figure 17 shows the conductivity measured at different frequencies from 20 Hz to 1 MHz for the PVA/AniHCl composites with different concentrations of AniHCl. At low AniHCl concentrations both the dc and ac conductivity are clearly seen. The dc conductivity is frequency-independent served by weakly bound electrons, H$^+$, and Cl$^-$ and those of phonon assisted tunneling process that gain charge mobility at room temperature. The H$^+$ and Cl$^-$ ions were derived from dissociation of HCl which is weakly attached to the phenyl group of aniline monomer. The ac conductivity at high frequencies is due to trapped H$^+$ and Cl$^-$ ions in PVA matrix that required alternating electric field at given frequency and contributes to the conductivity by hopping between the localized sites.

The conductivity increases with the increase of AniHCl concentration until 28.6 wt% before the conductivity drops to the lower values at higher concentrations of 33.0 and 38.0 wt%. The conductivity of higher concentrations is mainly the dc conductivity contributed from weekly bound H$^+$ and Cl$^-$ ions.

Figure 18 shows the dc conductivity component at various AniHCl monomer concentrations. The conductivity increases significantly from 6.61×10^{-8} S/m at 0 wt% to 1.04×10^{-4} S/m at 28.6 wt% and there is subsequently dropped in conductivity at 33.0 wt% and 38.0 wt%. A decrease in conductivity may be due to the increase of crystallinity in the polymer matrix as more crystalline chlorine are present within the composite films. It may also be due to high viscosity and caused resistance or impedance to oppose ion mobility in
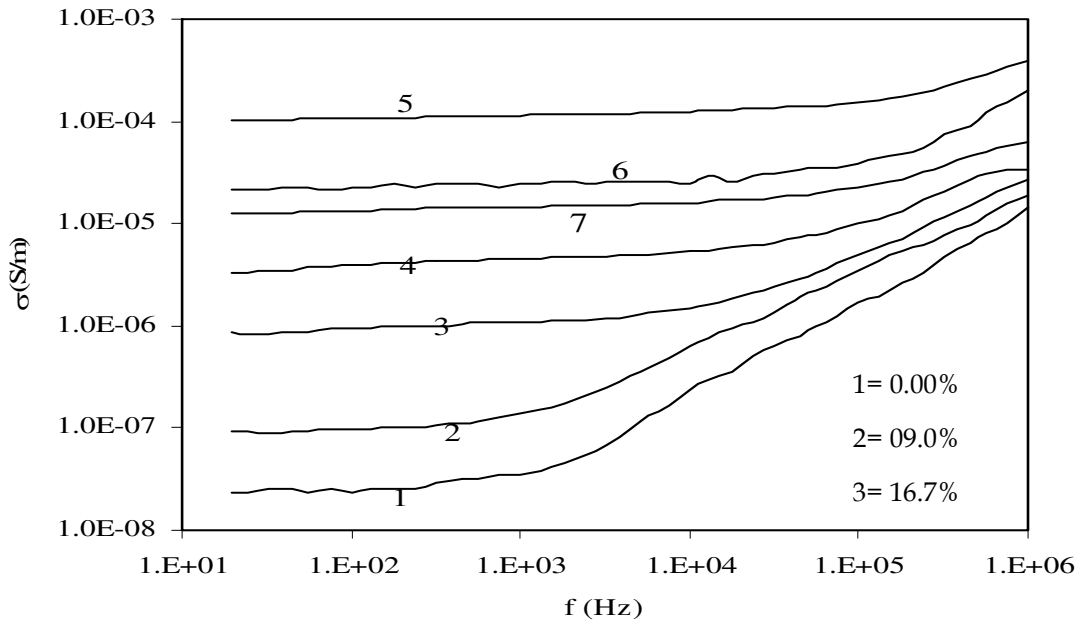
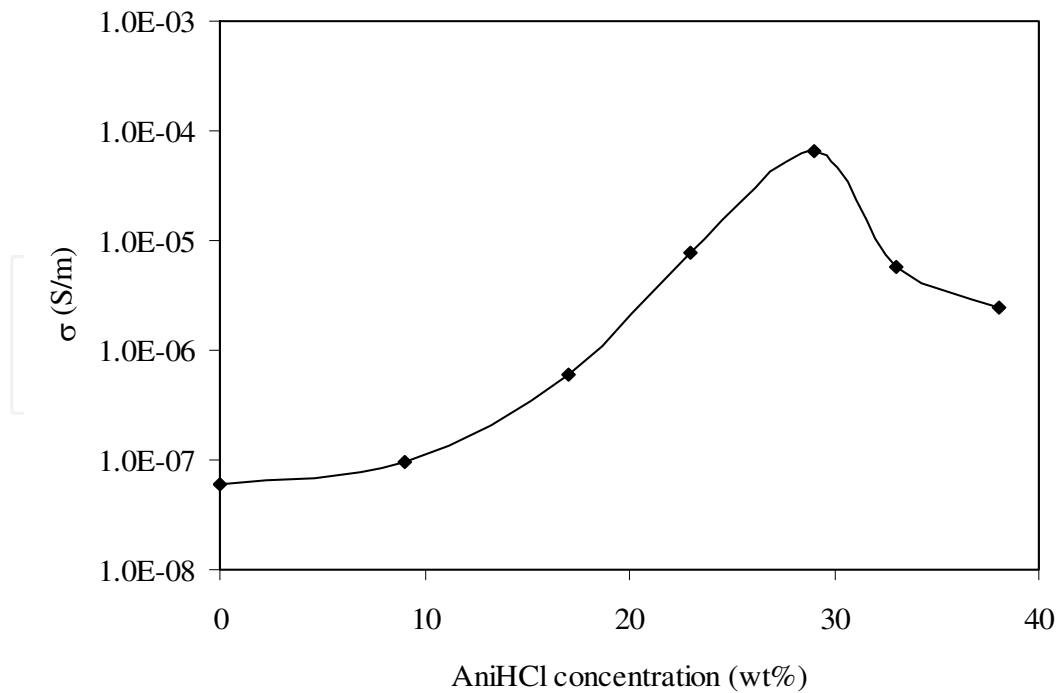Fig. 17. Conductivity of the PVA/AniHCl composites versus frequency at different concentrations of AniHCl.

Fig. 18. The dc conductivity of PVA/AniHCl composites vs. AniHCl monomer concentration.

the composites (Guo *et al.*, 2004; Bidstrup, 1995). It has been shown that the ionic mobility is inversely proportional to viscosity as in the theoretical relation given by Richard (2002). For this reason, the conductivity of PVA/AniHCl composites decreased in values at monomer concentrations of 33.0 and 38.0 wt%. Subsequently, the analysis of these samples was discarded from the further discussion.

16. Conductivity of PANI composites at various doses

Figure 19 shows the conductivity of PANI composites dispersed in PVA matrix polymerized at doses up to 50 kGy for various AniHCl concentrations from 9.0 to 28.6 wt%. The results show that the conductivity increases with the increase of dose and monomer concentration. As the dose and AniHCl concentration increased more polarons were formed and thus, increase the conductivity of conducting PANI composites. Moreover, as the dose increased the band gap of conducting PANI decreases to about 1.0 eV for 28.6 wt% AniHCl concentration and radiation dose at 50 kGy. This is closed to the silicon semiconductor band gap of about 0.8 eV. The conductivity comprises of the dc and ac components given equation (6).

$$\sigma(\omega) = \sigma_{dc}(0) + \sigma_{ac}(\omega) \tag{6}$$

At low doses below 10 kGy, the composites behave like insulators, where the dc and ac components are due to weakly bound and trapped H^+ and Cl^- ions in PVA/AniHCl matrix respectively. The ac conductivity at higher doses follows the universal power law of the form $\sigma_{ac}(\omega) = A\omega^s$ (Johnscher, 1976). Since the ac component is limited to the lower concentrations of AniHCl and at lower doses as shown in Figure 18, we suspected that the conductivity is not related to polarons in this situation. The ac component occurs at higher frequency region and becomes less important at higher doses. This indicates that at higher doses the conductivity is dominated entirely by the dc conductivity due to polarons. Therefore, detail analysis of the ac conductivity will not be discussed further. The species of polarons are considered the main criteria of conducting polyemeraldine salt that results in a remarkable shift of the dc conductivity to higher values with increasing dose and monomer concentration up to 28.6 wt%. Detail analysis of the dc conductivity is given in the following subsection.

17. The dc conductivity of PANI composites determined from direct extrapolation method

The dc conductivity $\sigma_{dc}(0)$ of conducting PANI composites was deduced from direct extrapolation of dc portion Figures 19 and from calculation using the resistance Z_0 obtained from the Cole-Cole plots. Figure 20 shows the dc conductivity $\sigma_{dc}(0)$ of PANI composites deduced by the direct extrapolation. We found that the dc component for 9 wt% AniHCl monomer increases from 6.31×10^{-7} S/m at 0 kGy to 1.12×10^{-3} S/m at 50 kGy, while for 16.7 wt % monomer, the dc conductivity increases from 3.63×10^{-6} S/m at 0 kGy up to 5.75×10^{-3} S/m at 50 kGy. As for 23 wt % monomer the conductivity increases from 4.02×10^{-6} S/m at 0 kGy to 2.40×10^{-2} S/m at 50 kGy. The highest conductivity measured
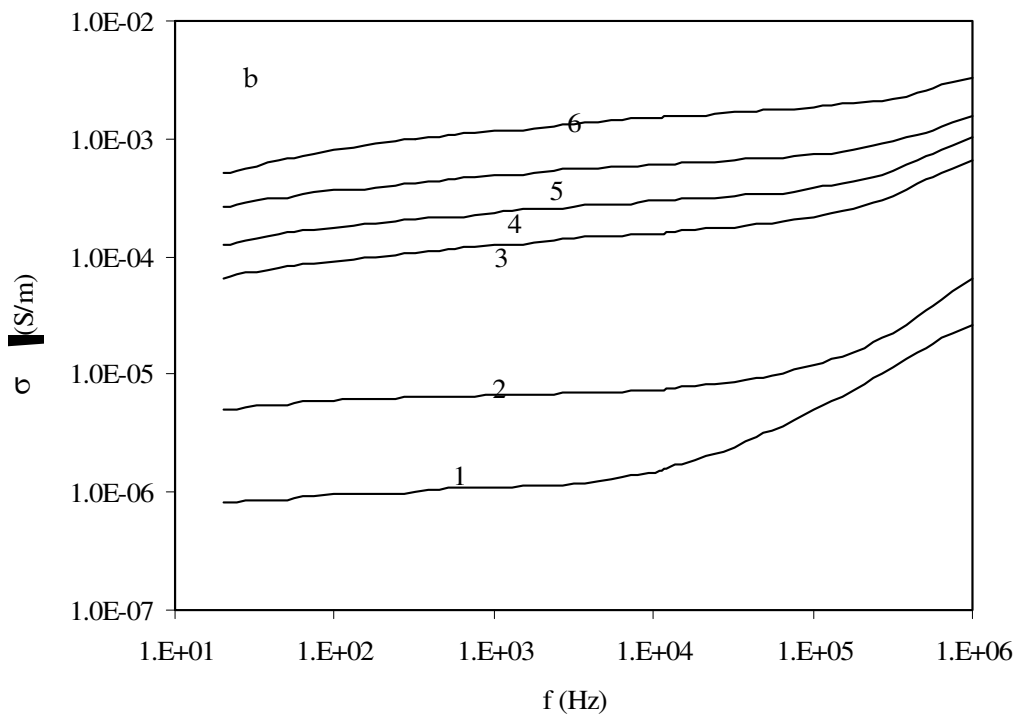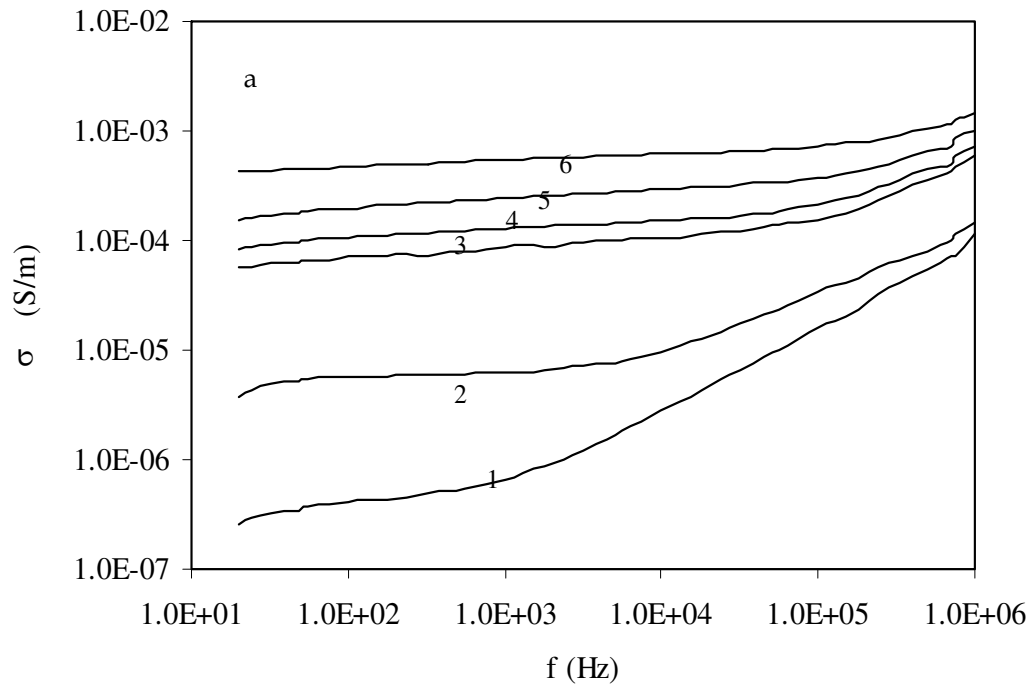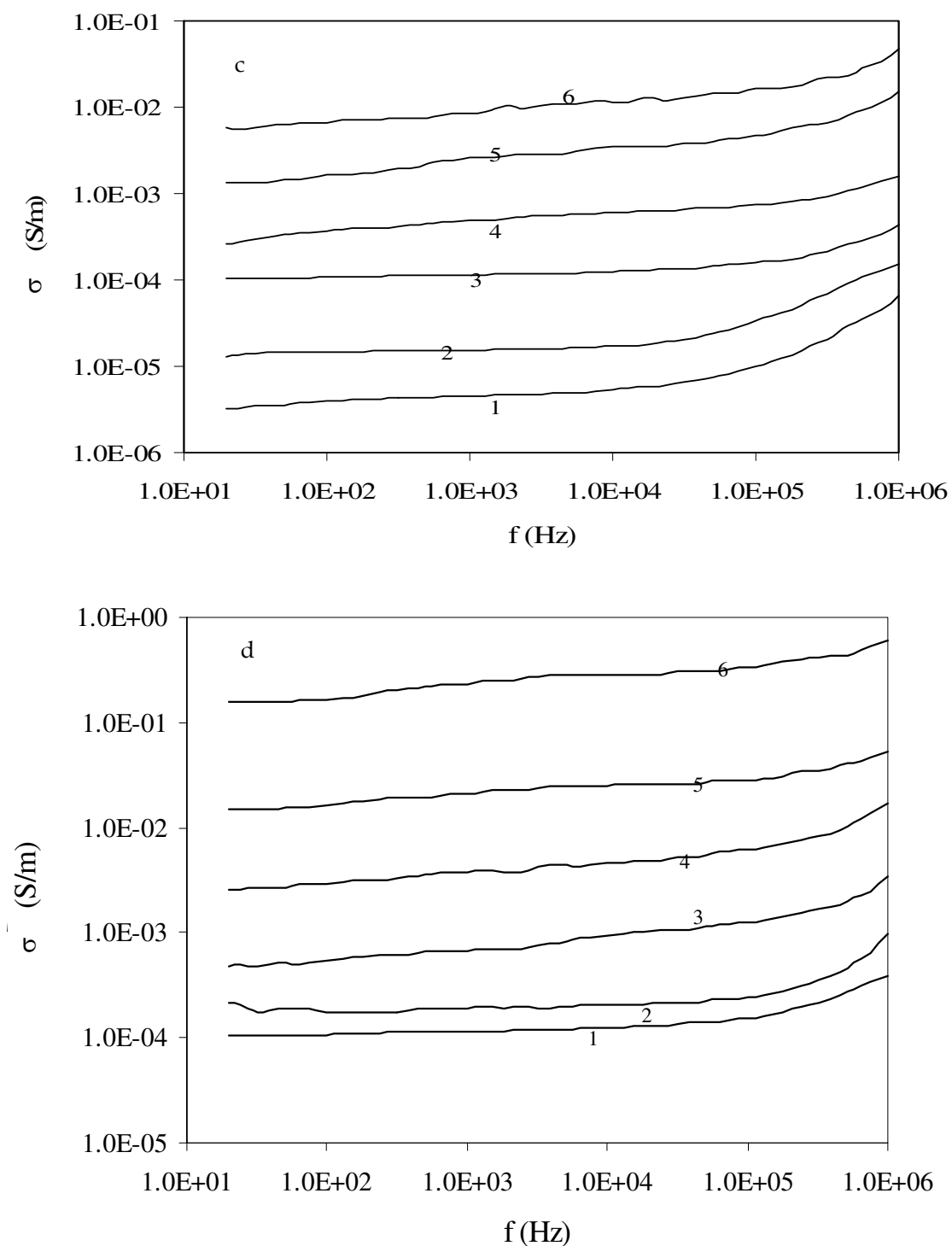
Fig. 19. Shows the conductivity vs. frequency of PVA/PANI nanocomposites irradiated up to 50 kGy for various monomer concentrations (a) 9.0, (b) 16.7, (c) 23.0, and (d) 28.6 wt%.

was for 28.6 wt % monomer at which the dc conductivity increases from 1.04×10^{-4} S/m at 0 kGy up to 1.17×10^{-1} S/m at 50 kGy. The obtained values were compared with previously published data for chemical and electrochemical doping methods. MacDiarmid *et al.* (1987) have successfully prepared conducting PANI by HCl doping and obtained a conductivity of 1.0 S/cm or $1.0 \times 10^{+2}$ S/m. Recently Blinova *et al.*, (2006) have successfully measured the conductivity of 15.5 S/cm or $1.55 \times 10^{+3}$ S/m for PANI prepared by chemical doping with 1 M phosphoric acid. The PVA/PANI-HCl composites of polyaniline were prepared and the maximum conductivity achieved was 2.0×10^{-3} S/m at 60 wt% PANI (Cho *et al.*, 2004). The difference in conductivity between PANI-Radiation doping and PANI-(chemical/electrochemical doping) is that radiation interaction occurs randomly i.e. not all AniHCl got polymerized and the effect of binder impedance.
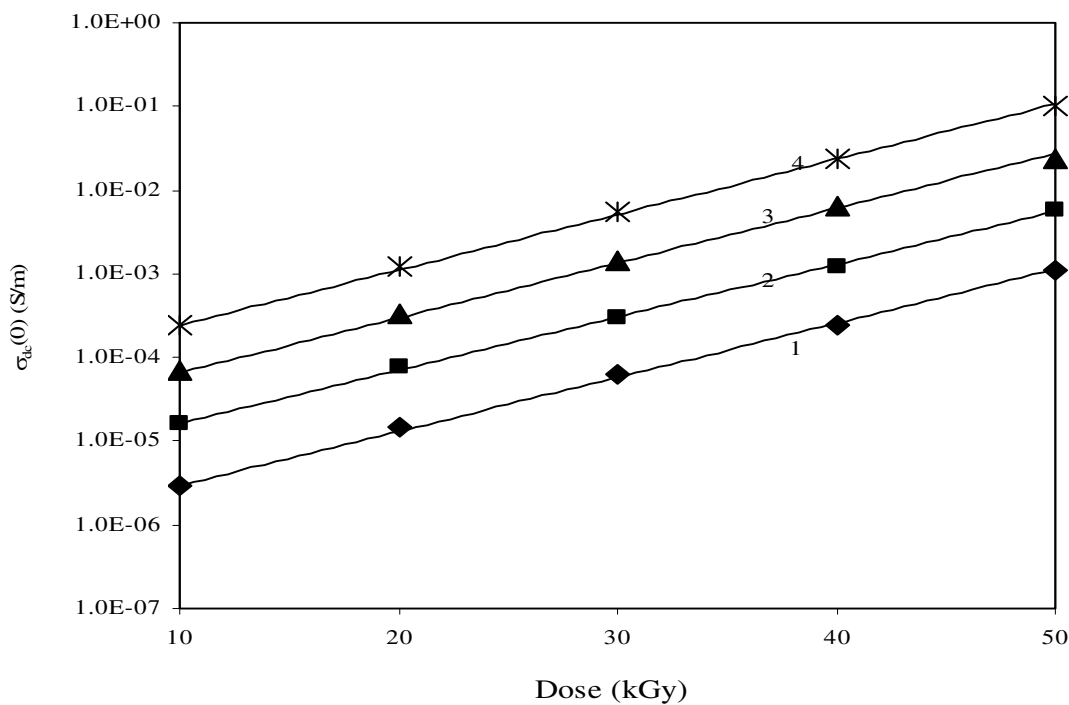
Fig. 20. Shows the dc conductivity $\sigma_{dc}(0)$ by extracted from extrapolation method for PANI composites in PVA matrix at different doses and monomer concentrations.

The dc conductivity of conducting PANI composites seems to begin at dose of 10 kGy. Referring to the absorption spectra Figure (2), the absorbance at 790 nm band for conduction PANI showed up at 10 kGy for all monomer concentrations, confirming that the formation of PANI begins at 10 kGy as measured by conductivity measurement. This minimum dose might be the threshold of radiation dose to start polymerizing the conducting PANI for all AniHCl concentrations. The general relationship between the dc conductivity and the dose is in the form: $\sigma_{dc}(0) = \sigma_0 \exp(D / D_0)$, D_0 is the dose sensitivity that can be deduce from the gradient linear slope of $\ln \sigma_{dc}(0)$ versus dose.

18. The dc conductivity of PANI determined from the Cole-Cole plots

The dc conductivity, $\sigma_{dc}(0)$ can be calculated from the resistance Z_0 obtained from the Cole-Cole plots. Figure 21 shows the Cole-Cole plot curves for various AniHCl monomer concentrations that display similar semicircle characteristics, a typical impedance spectra of synthetic-metal or metallic-polymer film composites (Vorotyntsev *et al.*, 1999; Tarola, *et al.*, 1999). At low frequency region for certain dose and monomer concentration, there is a straight line spike due to interstitial effect of the electrodes. It has been reported by Mariappan and Govindaraj. (2002) that the depressed semicircle at the low frequency region is related to characteristics of parallel combination of the bulk resistance and capacitance phase element of the samples. While Chen *et al*. (2003) ascribed the presence of straight line at low frequency region due to the capacitive characteristics of conducting polymer film.
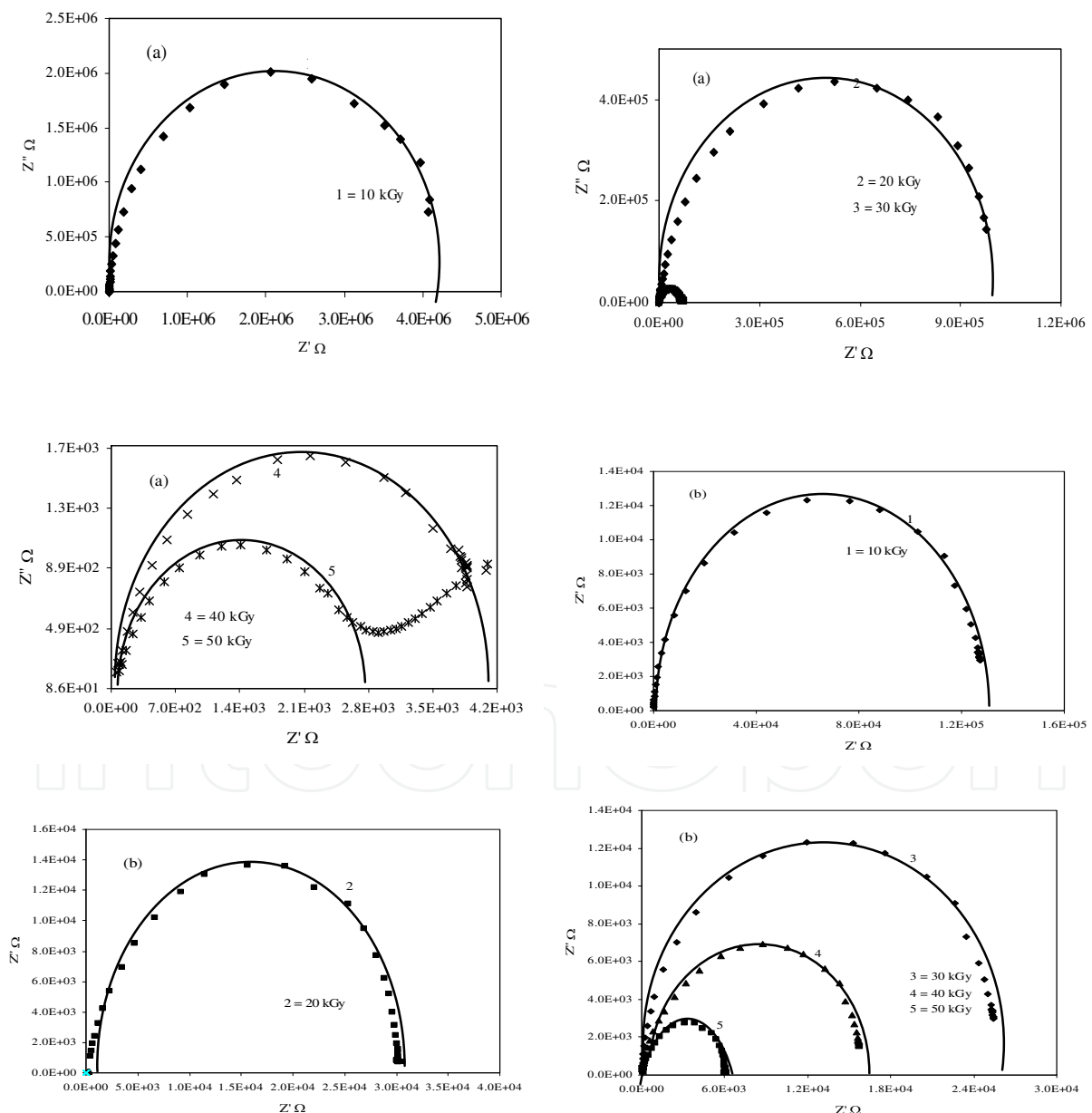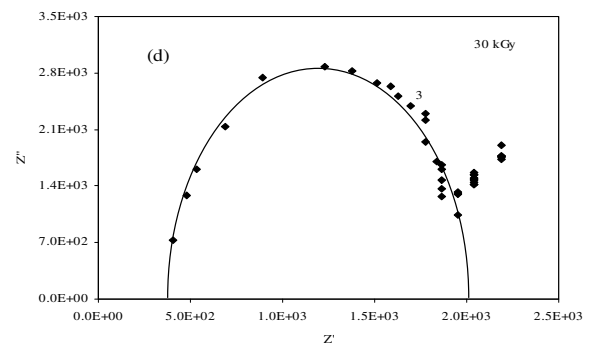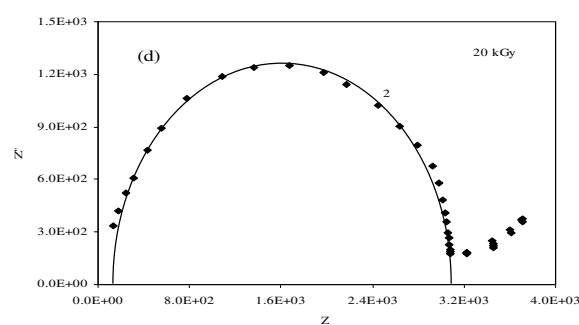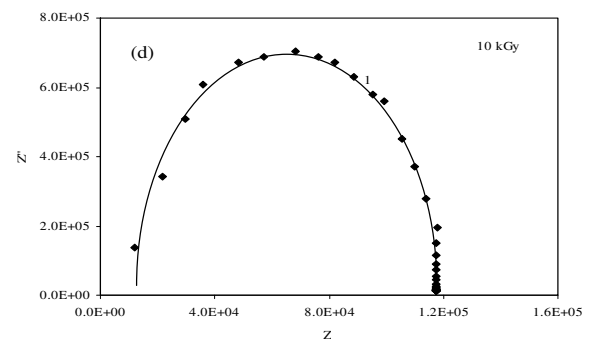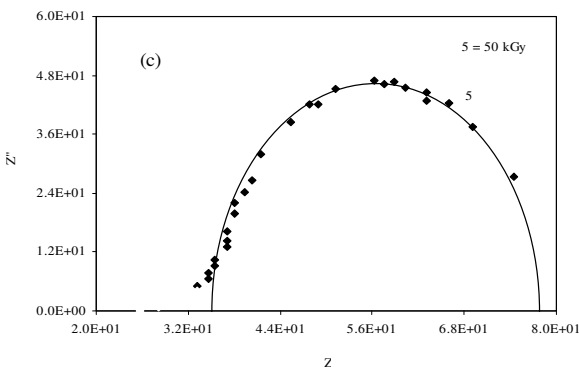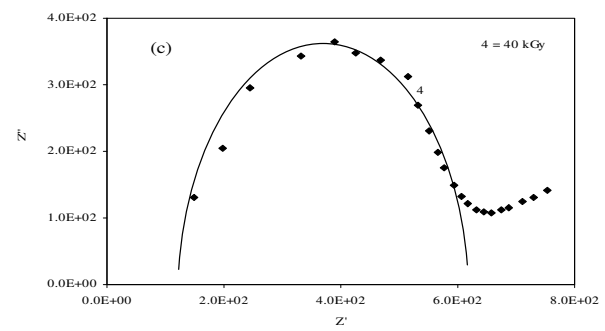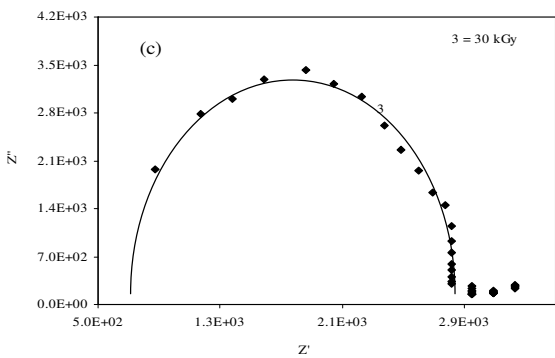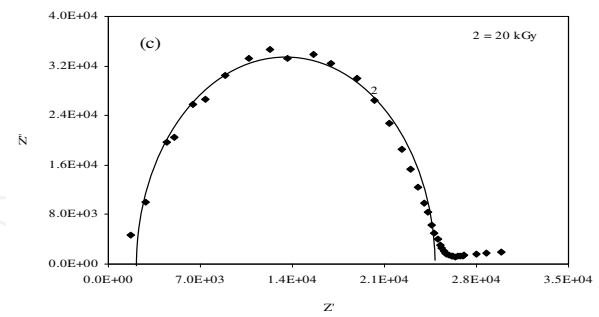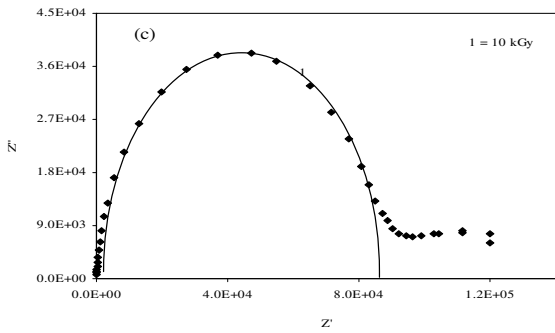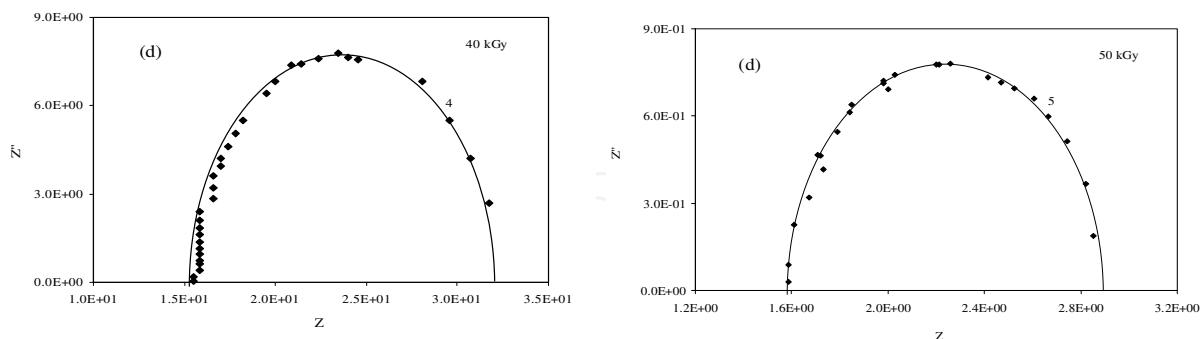
Fig. 21. Shows the Cole-Cole plots for PANI nanoparticles in PVA matrix at (a) 9 wt %, (b) 16.7 wt %, (c) 23 wt % and (d) 28.6 wt % of AniHCl monomer.

In such spectra the semicircles radius decreases with dose increment, indicating that the resistance Z_0 of the polymer composites decreases with dose, hence the dc conductivity $\sigma_{dc}(0)$ increases with dose (Kobayashi *et al.*, 2003). The increase of dc conductivity of the PANI composites is due to polaron species caused by γradiation beginning at 10 kGy. The inclined straight line appear at the end of the semicircles was due to electrode polarization or space effect (Hodge *et al.*, 1976 and Mariappan and Govindaraj., 2002), while Lewandowski *et al.* (2000) ascribed it to non secured verticality of electrode spikes as well as to capacitance interface between the electrode and the dielectric.

We found that the dc conductivity obtained from the Cole-Cole plots are quite typical with those deduced from the direct extrapolation method. The dc conductivity is 5.75×10^{-6} S/m at 10 kGy and 1.32×10^{-3} S/m at 50 kGy for 9.0 wt %. It is 1.0×10^{-5} S/m at 10 kGy and 2.95×10^{-3} S/m at 50 kGy for 16.7 wt %, while for 23.0 wt % it is 2.40×10^{-5} S/m at 10 kGy and 1.26×10^{-2} S/m at 50 kGy. For the concentration of 28.6 wt% it is 7.76×10^{-5} S/m at 10 kGy and 1.17×10^{-1} S/m at 50 kGy. The results are slightly different from the values determined by the extrapolating method. Previously Dutta, *et al.* (2001) measured ac and dc conductivity of chemically doped PVA/PANI blends and obtained the highest dc conductivity of 4.8×10^{-2} S/m.

Figure 22 shows the dc conductivity $\sigma_{dc}(0)$ versus radiation dose of conducting PANI composites for different monomer concentrations. The relation between the radiation dose D and the dc conductivity $\sigma_{dc}(0)$ can be fitted to the empirical exponential relation of the form $\sigma_{dc} = \sigma_0 \exp(D / D_0)$ where, σ_0 is the conductivity at zero doses, D is the absorbed dose and D_0 is the dose sensitivity of the composites to radiation effect. In order to determine the dose sensitivity D_o of the composites for irradiation, we followed 'Arrhenius type' plot of $\ln \sigma_{dc}$ versus dose, as the gradient of the linear regression plot gives $1 / D_0$, where D_0 is the dose sensitivity of the composites.
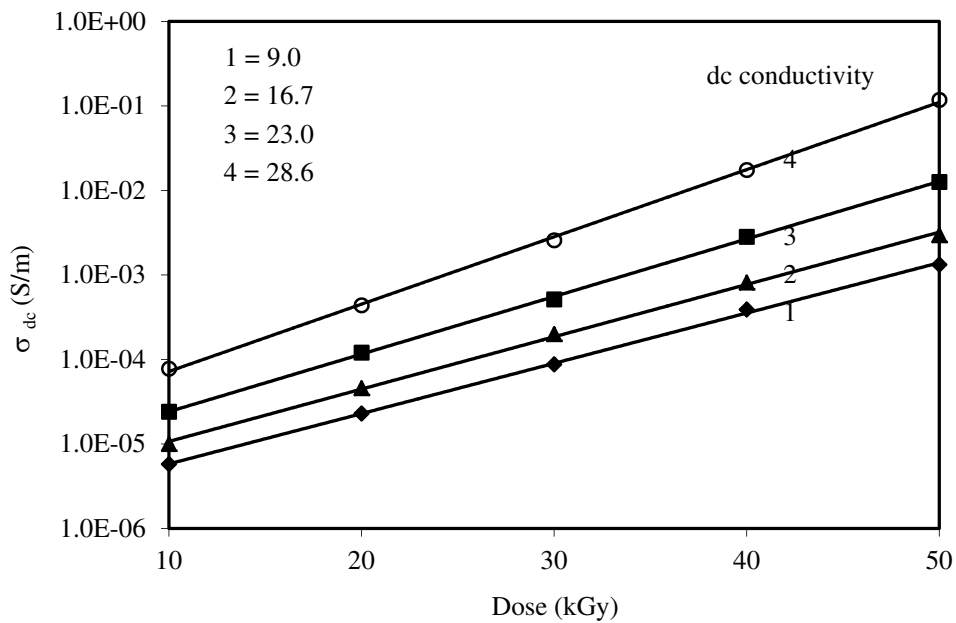
Fig. 22. Shows the dependence of dc conductivity (σ_{dc}) on the applied radiation dose theoretical method. The conductivity obeys the relation of the following form

$$\sigma_{dc} = \sigma_0 \exp(D / D_0)$$

Figure 23 shows the variation of $\ln \sigma_{dc}(0)$ as a function of dose for different monomer concentration of PANI nanoparticles. The linear regressions of the "Arrhenius type plot" $\ln \sigma_{dc}(0)$ versus dose give the slope of $1 / D_0$ from which the dose sensitivity value can be determined, as shown in Table 4. The study reveals that as the monomer concentration increases the dose sensitivity decreases.
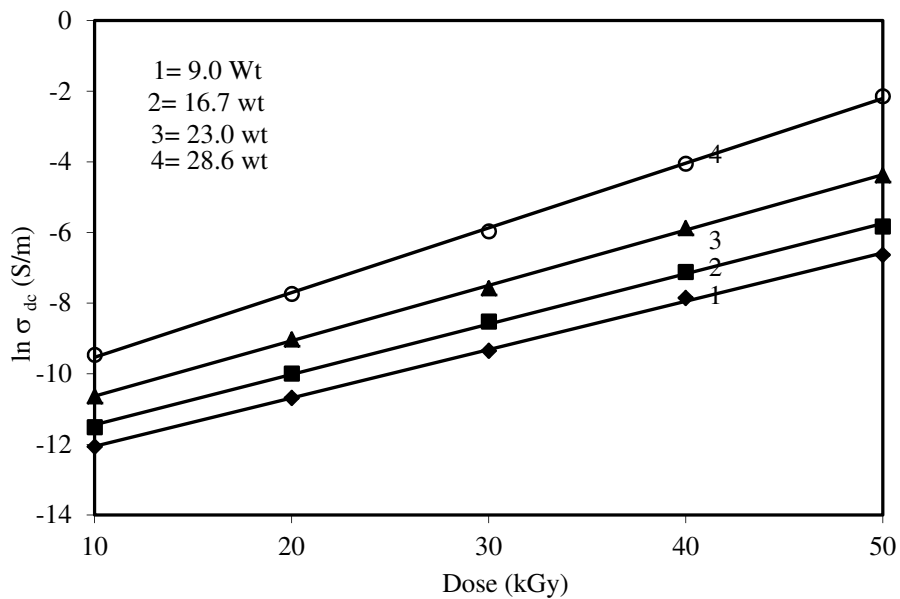

Fig. 23. Shows the variation of ln $\sigma_{dc}(0)$ versus radiation dose for different AniHCl concentration by theoretical method.

AniHCl concentration (Wt %)	D_0 (the Cole-Cole method) (kGy)	D_0 (extrapolating method) (kGy)
9.0	7.3	7.3
16.7	7.0	6.8
23.0	6.7	6.1
28.6	5.6	5.7

Table 4. Shows the relation between monomer concentration and dose sensitivity D_0

Figure 24 shows the dose sensitivity versus AniHCl concentration which reveals a decrease in dose sensitivity with the increase of monomer concentration i.e. as the dose increases the composites become more radiosensitive to produce conducting PANI nanoparticles. The correlation between the dose sensitivity and the concentration of monomer is given by the formula: $D_0 = -5.1C + 7.8$, where C refers to the AniHCl concentration. The increasing of radiosensitivity by increasing the AniHCl concentration is attributed to higher density of the monomer to be irradiated, thus, producing more polarons in conducting PANI.
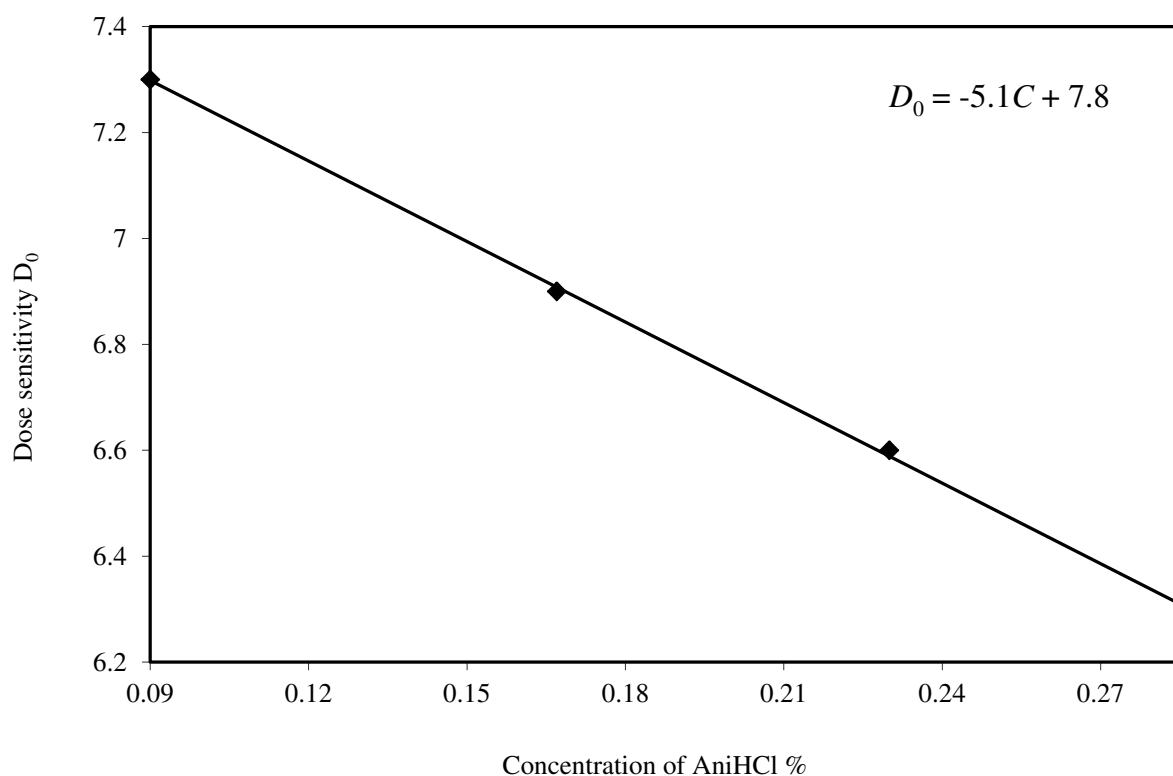

Fig. 24. Shows the variation of dose sensitivity D_0 versus the concentration of AniHCl within the PVA film by theoretical method.

18. Raman scattering analysis of PANI nanoparticles

The Raman scattering analysis was performed on the PVA/PANI nanocomposites before and after γ-irradiation up to 50 kGy and for all monomer concentrations. The significant of Raman spectroscopy study is that it can be used to investigate particular covalent bonds of some molecular species where the amount is expected to change after γ-irradiation. In this

method, the vibrational transitions of particular molecular bonds could provide information on the chemical structure of the materials, which might be modified by ionizing radiation. Thus, Raman scattering (inelastic scattering) method is vital for the identification of substances by targeting at particular bonds which can become a chemical finger printing and provide quantitative information of the samples of interest (Barnes, 1998).

Figure 25 shows Raman spectra of 28.6%-AniHCl composites of PVA/PANI composites at different doses and reveal the prominent peak originated at Raman shift 1637 cm^{-1} assigned to C=N bond stretching of imines group which gives the PANI color and represents the polaron species. In addition to the formed polarons of imines group, the Raman spectra also show Raman shift at 2100 cm^{-1} and 2527 cm^{-1} assigned for the π-bonds between double bond carbon C=C stretching within the aromatic ring and C=O stretching of aldehyde derivative from PVA bond scission respectively. Also shown is the weak intensity of Raman shift 3023 cm^{-1} assigned to C-H bending.
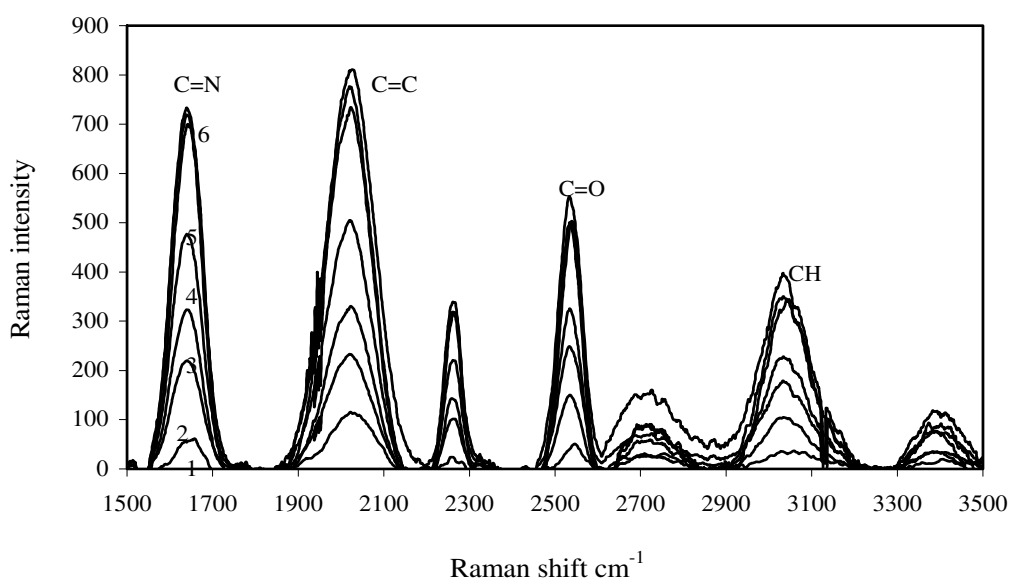

Fig. 25. Shows the Raman spectra showing Raman shifts of covalent bond species in the 28.6%-AniHCl nanocomposites of PVA/PANI nanoparticles induced by radiation doping at different doses

19. The SEM morphology of PANI nanoparticles

The morphology and particle size of the conducting PANI nanoparticles were studied by means of a scanning electron microscope (SEM). Figure 26 shows the SEM image of PANI nanoparticles polymerized 'in situ' by radiation doping with the dose of 50 kGy for AniHCl concentration of 28.6 wt%. The micrograph was taken at the electron operating voltage of 15 kV and 10,000 times magnification. It reveals the formation of conducting PANI nanostructures distributed almost uniformly and the diameter of spherical PANI nanoparticles was estimated to be in the range of 50 – 100 nm. The micrograph also reveals some fibrous clusters made up from aggregates of many PANI nanoparticles. The PANI cluster size is about 100 – 200 nm in diameter and 300 – 400 nm in length. There have been reported that the diameters of the PANI nanoparticles polymerized chemically with

hydrochloric acid were about 100 to 150 nm for PVA/PANI nanocomposites (Cho *et al.*, 2004) and 40 nm for PVP/PANI nanocomposites (Dispenza *et al.*, 2006). This suggests that the type of binder determined the diameter of spherical nanoparticles.
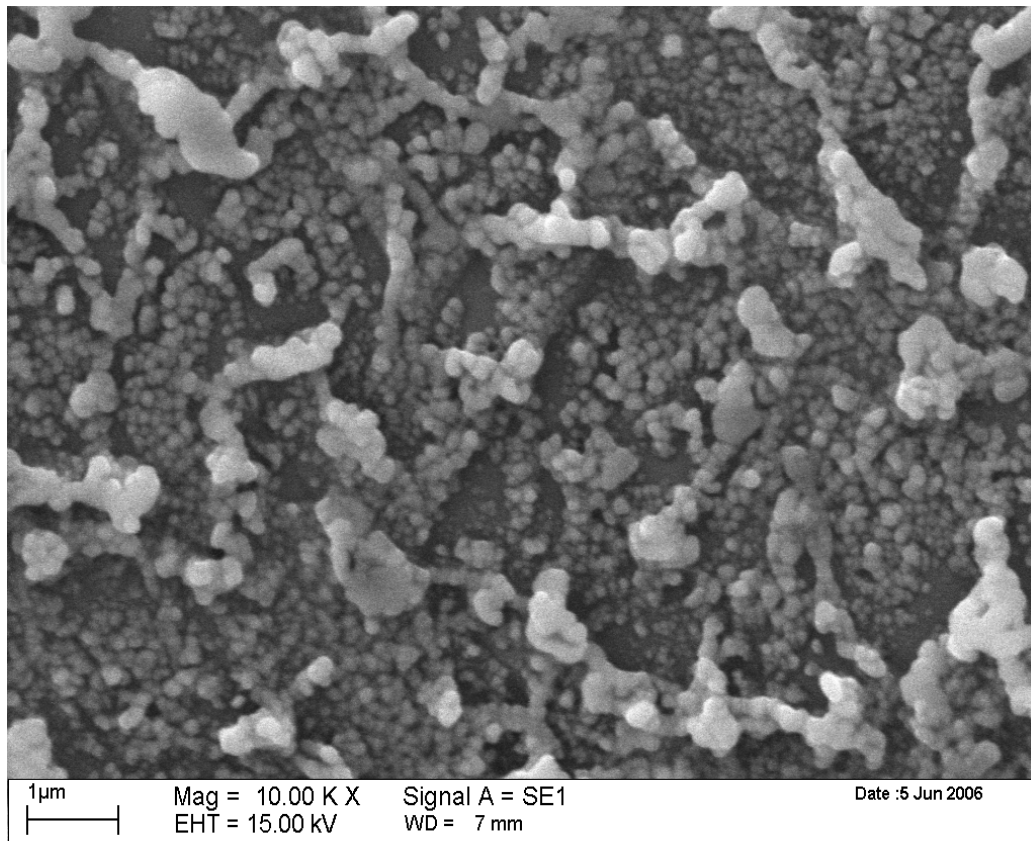

Fig. 26. Shows SEM image of PANI nanoparticles polymerized by 50-kGy Co-60 γ-rays for 28.6 wt% monomer.

The formed pallets of pure PANI-HCl (Fig. 1) were characterized with Voltmeter and LCR-meter. It is conductivity was obviously higher than that of PVA\PANI-HCl, which is ascribed to the presence of PVA within the composites, the conductivity was 1 S/m and it is UV-spectrum was peaked at 790 nm which is same as in PANI\PVA composites.

20. Conclusion

The ionizing γ-radiation could be used successfully to obtain the polymerization of monomers such as aniline hydrochloride AniHCl and the induced properties for the new product could be controlled by adjusting the amount of monomers and the applied radiation dose with consideration to technical aspects.

21. References

Albuquerque, J.E. de, L.H.C. Mattoso, R.M. Faria, J.G. Masters and A.G. MacDiarmid. 2004. Study of the interconversion of polyaniline oxidation states by optical absorption spectroscopy. *Synthetic Metals* 146, (1): 1-10.

Angelopoulos, J. M. Shaw, W. S. Huang and R. D. Kaplan. In-Situ Radiation Induced Doping. 1990. Molecular Crystal Liquid Crystal 189 No. 1: 221-225.

Arshak, A., S. Zleetni and S.K. Arshak. 2002. γ-irradiation sensor using optical and electrical properties of manganese phthalocyanine (MnPc). Thick Film Sensor 2: 174-184.

Azian, Osman. 2006. Ionizing Radiation Effects on Poly(Vinyl Alcohol)/(Aniline Hydrochloride blend Films. M.Sc. dissertation, Physics Department, UPM, Malaysia.

Barnes, A., A. Despotakis, P.V. Wright, T.C.P. Wong, B. Chambers, A.P. Anderson. 1998. Electrochim. Acta 43: 1629-1635.

Bidstrup, S., Simpson J. 1995. Light Scattering Study of Vitrification during the Polymerization of Model Epoxy Resins. Journal of Polymer Physics Ed. 33-43.

Blanco, J. F, Q. T. Nguyen, P. Schaetzel. 2001. Novel hydrophilic membrane materials: sulfonated polyethersulfone Cardo. Journal of Membrane Science186: 267-279.

Blinova, Natalia V., Jaroslav Stejskal, Miroslava Trchová and Jan Prokeš. 2006. Polyaniline prepared in solutions of phosphoric acid: Powders, thin films, and colloidal dispersions, Polymer 47 (1): 42-48.

Blythe, A.R. 1979. In Electrical Properties of Polymers. Cambridge university Press P. 90.

Bodugoz, H. Sevil, U. A. Güven O. 1998. Radiation induced conductance in blends of poly(aniline-base) with poly(vinyl chlrodie)-co(vinyl acetate). Macromolecule Symposium 169: 289-295.

Chen, W.C., T.C. Wen, H.S. Teng. 2003. Polyaniline-deposited porous carbon electrode for supercapacitor. Electrochim. Acta 48: 641-649.

Cho, Min, Seong, S.Y. Park, J.Y. Hwang, H.J. Choi. 2004. Synthesis and electrical properties of polymer composites with polyaniline nanoparticles. Material Science Engineering C 24: 15-18.

Denaro, A. R. and Jayson, G. G. 1972. Fundamental of radiation chemistry. Butterworths, London.

Dispenza, C., M. Leone, C.Lo. Presti, F. Librizzi, G. Spadaro, V. Vetri. 2006. Optical properties of biocompatible polyaniline nano-composites. Journal of Non-Crystalline Solids 352: 3835–3840.

Dutta, P., Biswas S., Ghosh M., De S. K., Chatterjee S. 2001. The dc and ac conductivity of the polyaniline-polyvinyl alcohol blends. Synthetic Metals 122: 455-461.

El-Sayed, S., M., Arnaoutry M. B., Fayek S. A. 2003. Effect of grafting, gamma irradiation and light exposure on optical and morphological properties of grafted low density polyethylene films. Polymer Testing 22: 17-23.

Guo, Z., J. Warner, P. Christy, D. E. Knanbuehl, G. Boiteux, G. Seytre. 2004. Ion mobility time of flight measurements: isolating the mobility of charge carriers during an epoxy-amine reaction. Polymer 45: 8825-8835.

Hodge, IM, M. D. Ingram, A. R. West. 1976. Impedance and modulus spectroscopy of polycrystalline solid electrolytes. Journal of Electroanalytical Chemistry, 74: 125-143.

Johnsher, A., K., M. S. Frost, 1976. Weekly frequency dependant of electrical conductivity in chalogenide glass. Thin solid films, 37, 103-107.

Johns, H., E., J.R. Cunningham. 1983. The Physics of Radiology, fourth ed., Thomas, Sprinfield, IL.

Kanazawa K. K., A. F. Diaz, R. H. Geiss, W. D. Gill, J.F. Kwak, J.A. Logan, J.F. Rabolt and G.B. Street. 1980. J. Chem. Soc. Chem. Commun. 854.

Kobayashi, N., Chinone H., Miyazaki A. 2003. Polymer electrolyte for novel electrochromic display. Electrochimica Acta 48: 2323-2327.

Lewandowski, A., Skorupska K., Malinska J. 2000. Novel (polyvinyl alcohol) –KOH-H2O alkaline polymer electrolyte. Solid state ionic 133: 265-271.

Lokhovitsky, V.I. and V.V. Polikarpov. 1980. Technology of radiation emulsion polymerization. Atomizdat, Moscow-Russia.

MacDiarmid, A.G., J. Chiang, A.F. Richther. 1987. Polyaniline: a new concept in conducting polymers. Synthetic Metals 18: 285-290.

Malmonge, J A, Mattoso L H C. 1997.Doping of polyaniline and derivatives induced by X-ray radiation. Synthetic Metals 84: 779-780.

Malinauskas A. Malinauskiene J. and Ramanavicius A. (2005). Conducting polymer-based nanostructurized materials: electrochemical aspects. Nanotechnology, 16: R51-R62.

Mariappan, C. R., Govindaraj G. 2002. Ac conductivity, dielectric studies and conductivity scaling of NASICON materials. Materials Science and Engineering B94: 82-88.

McGervey, J., 1983. Introduction to Modern Physics, 2nd. edition, Academic Press, New York.

Mohammed A. Ali Omer, Elias S., Khairulzaman Hj M. Dahlan. 2007. Radiation Synthesis and Characterization of Conducting Polyaniline and Polyaniline/silver nanoparticles. Ph. D. thesis, Physics Department, UPM, Malaysia.

Mott, N., F. and Davis E.A. 1979. Electronic Process in Non-crystalline Materials, 2nd. Edition. Clarendon Press, Oxford, UK.

Park, H. B., S. Y. Nam, J. W. Rhim, J. M. Lee, S. E. Kim, R. Kim, Y. M. Lee. 2002. Copolymerization of Styrene onto Polyethersulfone Films Induced By Gamma Ray Irradiation. Journal of Applied Polymer Science 86: 2611-2614.

Rao, P. S., Anand J., Palaniappan S. and Sathyanarayana D. N. 2000. European Polymer Journal 36: 915-920.

Richard, A., Pethrick, David Hayward Pro. 2002. Study of ageing of adhesive bonds with various surface treatments. Polymer Science 27: 1983 – 2017.

Sevil, U. A., O. Güven, A. Kovács, I. Slezsák. 2003. Gamma and electron dose response of the electrical conductivity of polyaniline based polymer composites. Radiation Physics and Chemistry 67: 575–580.

Siegbahn, K., 1965. Alpha, Beta and Gamma Ray Spectroscopy, North-Holland, Amsterdam, Netherlands.

Smith, F., A. 2000. A Primer in Applied Radiation Physics. World Scientific Publishing Co. Pte. Ltd.

Tarola, A., D. Dini, E. Salatelli, F. Andreani, F. Decker. 1999. Electrochemical impedance spectroscopy of polyalkylterthiophenes. Electrochim. Acta 44: 4189-4193.

Vorotyntsev, M.A., J.P.Badiali, G. Inzelt. Electrochemical impedance spectroscopy of thin films with two mobile charge carriers: effects of the interfacial charging. 1999. J. Electroanal.Chem. 472: 7-19.
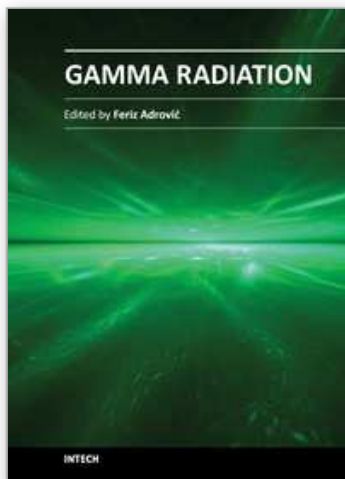
Gamma Radiation

Edited by Prof. Feriz Adrovic

This book brings new research insights on the properties and behavior of gamma radiation, studies from a wide range of options of gamma radiation applications in Nuclear Physics, industrial processes, Environmental Science, Radiation Biology, Radiation Chemistry, Agriculture and Forestry, sterilization, food industry, as well as the review of both advantages and problems that are present in these applications. The book is primarily intended for scientific workers who have contacts with gamma radiation, such as staff working in nuclear power plants, manufacturing industries and civil engineers, medical equipment manufacturers, oncologists, radiation therapists, dental professionals, universities and the military, as well as those who intend to enter the world of applications and problems of gamma radiation. Because of the global importance of gamma radiation, the content of this book will be interesting for the wider audience as well.

INTECH
open science | open minds